

# PCCP

Accepted Manuscript



This is an *Accepted Manuscript*, which has been through the Royal Society of Chemistry peer review process and has been accepted for publication.

*Accepted Manuscripts* are published online shortly after acceptance, before technical editing, formatting and proof reading. Using this free service, authors can make their results available to the community, in citable form, before we publish the edited article. We will replace this *Accepted Manuscript* with the edited and formatted *Advance Article* as soon as it is available.

You can find more information about *Accepted Manuscripts* in the [Information for Authors](#).

Please note that technical editing may introduce minor changes to the text and/or graphics, which may alter content. The journal's standard [Terms & Conditions](#) and the [Ethical guidelines](#) still apply. In no event shall the Royal Society of Chemistry be held responsible for any errors or omissions in this *Accepted Manuscript* or any consequences arising from the use of any information it contains.

## On the mechanism of cold denaturation

**Giuseppe Graziano**

Dipartimento di Scienze e Tecnologie, Università del Sannio

Via Port'Arsa 11 – 82100 Benevento, Italy

Phone: +39/0824/305133; Fax: +39/0824/23013

E-mail: [graziano@unisannio.it](mailto:graziano@unisannio.it)

### Summary

A theoretical rationalization of the occurrence of cold denaturation for globular proteins was devised, assuming that the effective size of water molecules depends upon temperature [G. Graziano, *Phys.Chem.Chem.Phys.*, 2010, **12**, 14245-14252]. In the present work, it is shown that the latter assumption is not necessary. By performing the same type of calculations in water, 40% (by weight) methanol, and carbon tetrachloride, it emerges that cold denaturation occurs only in water due to the special temperature dependence of its density and the small size of its molecules. These two coupled factors determine the magnitude and the temperature dependence of the stabilizing term that measures the gain in configurational/translational entropy of water molecules upon folding of the protein. This term has to be contrasted with the destabilizing contribution measuring the loss in conformational entropy of the polypeptide chain upon folding.

## Introduction

It is well established that the folded state of globular proteins is denatured by both increasing the temperature (i.e., hot denaturation) and lowering the temperature (i.e., cold denaturation).<sup>1,2</sup> Cold denaturation is a strange phenomenon because it is characterized by a decrease in both enthalpy and entropy, even though the disorder of the polypeptide chain increases. A rationalization of the occurrence of cold denaturation can shed light on the molecular details of the conformational stability of the folded state. I have devised a simple theoretical rationalization of cold denaturation grounded on the basic notion that the difference in solvent-excluded volume effect due to the different shape of the folded state with respect to the unfolded one plays a pivotal role.<sup>3,4</sup> An explanation of the meaning of the solvent-excluded volume effect is necessary. The creation of a cavity, at constant temperature and pressure, causes an increase of the liquid volume equal to the partial molar volume of the cavity itself and should not modify the volume packing density of the liquid. However, cavity creation, notwithstanding the volume increase, produces a geometric constraint for the liquid molecules: the centres of the latter cannot enter the shell between the van der Waals surface of the cavity and its solvent accessible surface. This geometric constraint produces a solvent-excluded volume effect (that can be measured by the solvent accessible surface area,<sup>5</sup> SASA, of the cavity), leading to a significant decrease in the total number of available configurations, and so to a loss of configurational/translational entropy of liquid molecules. This entropy loss is larger in water than in common organic solvents due to the small size of water molecules,<sup>6,7</sup> rules the poor solubility of nonpolar species in water (i.e., hydrophobic hydration), and is the physical basis for the association of nonpolar objects in water<sup>8</sup> (i.e., hydrophobic interaction).

The folding of globular proteins causes a large SASA decrease,<sup>9</sup> that translates in a large gain of configurational/translational entropy of water molecules.<sup>3,4</sup> More correctly, polypeptide chains are forced to assume a minimum SASA conformation to maximize this entropy. This is the right definition of intra-molecular hydrophobic interaction in protein folding. The entropy of water molecules, as originally proposed by Kauzmann,<sup>10</sup> is the driving force for the collapse of polypeptide chains. The entropy gain, however, is not due to

a reduction in the number of “icebergs” (i.e., an imagined increase in the order and strength of the H-bonded network surrounding nonpolar side chains); it is due to an increase in the available configurational space due to SASA reduction associated with folding. This entropic driving force acts as a “non-specific glue” because it is independent of the chemical nature of protein surface: SASA minimization is the consequence of the maximization of the configurational/translational entropy of water molecules for the given constraints of the system (i.e., a polypeptide chain in water). The solvent-excluded volume effect: (a) is a consequence of geometric properties of the whole conformation, and cannot be partitioned in additive group contributions; (b) has nothing to do with the chemical nature of solute-solvent interactions; (c) accounts for multi-particle correlations due to volume occupancy (both solvent-solvent and solute-solvent correlations); (d) is measured by calculating the reversible work to create a cavity suitable to host the given conformation (i.e., classic scaled particle theory,<sup>11</sup> SPT, grounded in statistical geometry,<sup>12</sup> is well suited for this task).

The large gain in configurational/translational entropy of water molecules is the main stabilizing contribution of the native state, and it overwhelms, over the temperature range where the native state is stable, the destabilizing contribution due to the polypeptide chain conformational entropy.<sup>3,4,13</sup> However, the gain in configurational/translational entropy of water molecules associated with the transition from unfolded conformations to the native state is a quantity that depends upon temperature. It has been shown that such a gain decreases significantly on lowering the temperature below 0 °C, paralleling the decrease in liquid water density.<sup>3,14</sup> At the temperature where the destabilizing contribution of the polypeptide chain conformational entropy exactly matches the stabilizing contribution of the water configurational/translational entropy, cold denaturation occurs. Therefore, the decrease in water density below 3.98 °C, the temperature of maximum density, TMD, together with the small size of water molecules, is a fundamental factor for the occurrence of cold denaturation.

Recently, Yoshidome and Kinoshita,<sup>15</sup> Y&K, pointed out that: (a) such rationalization is not strictly correct because the density decrease below TMD is not really important, at least up to -15 °C; (b) the main role in my approach is played by the temperature dependence of the effective diameter of water molecules, determined by fitting the experimental values of the

isothermal compressibility using a classic SPT formula.<sup>3</sup> In order to reply to such remarks, in the present work, it is shown that: (a) the devised approach produces cold denaturation also by considering temperature-independent the effective hard sphere diameter of water molecules; (b) the devised approach, by performing the same type of calculations, produces cold denaturation in water, but not in aqueous 40% (by weight) methanol solution, in methanol, and in carbon tetrachloride. The present results should confirm the rightness of the original rationalization of the mechanism of cold denaturation,<sup>3</sup> and the pivotal role played by the special temperature dependence of water density, determined, in turn, by the special features of H-bonds.

### Theory section

**A. Theoretical approach.** The unfolding of globular proteins in a solvent can be described as a conformational equilibrium,  $N \rightleftharpoons D$ , where N represents an average of the ensemble of native conformations (i.e., N-state), and D represents an average of the ensemble of denatured conformations (i.e., D-state). At equilibrium the chemical potentials of the two states have to satisfy the following relationship:

$$\mu_D = \mu_N \quad (1)$$

According to the general expression of the chemical potential derived from statistical mechanics,<sup>16</sup> by considering that the translational degrees of freedom can be treated classically, one has:

$$\mu_N = \mu_N^\bullet + RT \cdot \ln(\rho_N \Lambda_N^3) \quad (2)$$

$$\mu_D = \mu_D^\bullet + RT \cdot \ln(\rho_D \Lambda_D^3) \quad (3)$$

where  $\rho_N$  and  $\rho_D$  are the number densities of the N-state and D-state in the solvent,  $\Lambda_N$  and  $\Lambda_D$  are the momentum partition functions of the N-state and D-state;  $\mu_N^\bullet$  is the Ben-Naim

standard chemical potential of the N-state (i.e., transfer from a fixed position in the gas phase to a fixed position in the solvent<sup>17</sup>) and is given by:

$$\mu_N^\bullet = -RT \cdot \ln \langle \exp(-\Psi_N/RT) \rangle - RT \cdot \ln q_N \quad (4)$$

where  $\Psi_N$  is the perturbing potential due to the insertion of the N-state in the solvent, the ensemble average has to be taken over the pure liquid configurations,<sup>18</sup> and  $q_N$  is the internal partition function of the N-state, accounting for its roto-vibrational energy levels. By using Lee's expression of  $\Psi_N$ ,<sup>19</sup> one obtains:

$$\mu_N^\bullet = \Delta G_C(N|s) + E_a(N|s) - RT \cdot \ln q_N \quad (5)$$

where  $\Delta G_C(N|s)$  represents the reversible work to create in the solvent a cavity suitable to host the N-state, and  $E_a(N|s)$  represents the energetic interactions of the N-state with surrounding solvent molecules.

Similarly,  $\mu_D^\bullet$  is the Ben-Naim standard chemical potential of the D-state and is given by:

$$\mu_D^\bullet = -RT \cdot \ln \langle \exp(-\Psi_D/RT) \rangle - RT \cdot \ln \{ q_D \cdot \exp[-\Delta E(\text{intra})/RT] \} \quad (6)$$

where  $\Psi_D$  is the perturbing potential due to the insertion of the D-state in the solvent, the ensemble average has to be taken over the pure liquid configurations;<sup>18</sup>  $q_D$  is the internal partition function of the D-state, accounting for its roto-vibrational energy levels; and the exponential factor accounts for the fact that each internal energy state of the D-state has an additional energy with respect to the N-state due to the loss of inter-residue interactions (both H-bonds and van der Waals contacts) existing in folded conformations. By using Lee's expression of  $\Psi_D$ ,<sup>19</sup> one obtains:

$$\mu_D^\bullet = \Delta G_C(D|s) + E_a(D|s) + \Delta E_a(\text{intra}) - RT \cdot \ln q_D \quad (7)$$

where  $\Delta G_C(D|s)$  represents the reversible work to create in the solvent a cavity suitable to host the D-state, and  $E_a(D|s)$  represents the energetic interactions of the D-state with surrounding solvent molecules. It is worth noting that in eqns (5) and (7) terms due to the structural reorganization of solvent molecules upon solute insertion are not present because such a process is characterized by an almost complete enthalpy-entropy compensation,<sup>15,20-22</sup> and the corresponding Gibbs energy contribution can be neglected. By inserting eqns (2), (3), (5) and (7) into eqn (1), one obtains:

$$\begin{aligned} \Delta G_C(D|s) + E_a(D|s) + \Delta E(\text{intra}) - RT \cdot \ln q_D + RT \cdot \ln(\rho_D \Lambda_D^3) = \\ = \Delta G_C(N|s) + E_a(N|s) - RT \cdot \ln q_N + RT \cdot \ln(\rho_N \Lambda_N^3) \end{aligned} \quad (8)$$

that can be rearranged to:

$$\begin{aligned} [\Delta G_C(D|s) - \Delta G_C(N|s)] + [E_a(D|s) + \Delta E(\text{intra}) - E_a(N|s)] + \\ -RT \cdot \ln(q_D/q_N) + RT \cdot \ln(\Lambda_D^3/\Lambda_N^3) = -RT \cdot \ln(\rho_D/\rho_N) = -RT \cdot \ln K_D = \Delta G_D(s) \end{aligned} \quad (9)$$

where  $K_D = \rho_D/\rho_N$  is the equilibrium constant of the denaturation/unfolding equilibrium and  $\Delta G_D(s)$  is the standard denaturation Gibbs energy change in the solvent. Since the momentum partition functions of the N-state and D-state are identical, the corresponding term in eqn (9) proves to be zero and the latter can be re-written as:

$$\Delta G_D(s) = \Delta \Delta G_C(s) + \Delta E_a(s) - T \cdot \Delta S_{\text{conf}} \quad (10)$$

where the exact physical meaning of the  $\Delta \Delta G_C$  and  $\Delta E_a$  contributions is specified by the terms in the square brackets of eqn (9); and the ratio of the internal partition functions of the D-state and N-state has been assumed to represent the change in conformational entropy associated with protein unfolding (see Appendix A). Equation (10) corresponds to the expression obtained by means of a thermodynamic cycle approach;<sup>3</sup> the statistical mechanical derivation should strengthen its reliability.

I assumed that the algebraic sum of the three energetic terms in the expression of  $\Delta E_a(s)$  is zero in water,<sup>3,4</sup> because there should be an almost perfect balance for the energetic interactions between the D-state and the N-state, by taking into account both intra-protein interactions and those with water molecules (see Appendix B). To test the rightness of the proposed mechanism of cold denaturation, I assume that  $\Delta E_a(s)$  is zero also in the other considered solvents. So the  $\Delta G_d(s)$  expression is:

$$\Delta G_d(s) = \Delta \Delta G_c(s) - T \cdot \Delta S_{\text{conf}} \quad (11)$$

where the  $\Delta \Delta G_c(s)$  term always stabilizes the N-state, because it accounts for the configurational/translational entropy gain of solvent molecules associated with the SASA decrease upon folding, and the  $T \cdot \Delta S_{\text{conf}}$  term always stabilizes the D-state.<sup>3,23</sup> The  $T \cdot \Delta S_{\text{conf}}$  term is assumed to be independent of the solvent in which the globular protein is dissolved (i.e., it has the same value in water and in the other considered solvents). The allowed regions in the Ramachandran plot (strictly linked to the conformational degrees of freedom of the polypeptide chains) are mainly determined by steric constraints (i.e., the hard sphere sizes of the various groups), as originally pointed out by Ramachandran and colleagues and recently confirmed by Regan and colleagues.<sup>24</sup> This means that the value of the  $T \cdot \Delta S_{\text{conf}}$  term does not depend upon the solvent if the conformational transition involves the same two macrostates of the protein.

**B. Calculation procedure.** It is assumed, as in previous applications of this theoretical approach,<sup>3,4</sup> that: (1) The N-state can be represented as a simple sphere, whereas the D-state can be represented as a prolate spherocylinder, possessing the same  $V_{\text{vdW}}$  of the sphere representing the N-state,<sup>25</sup> but a markedly larger SASA (whose exact value depends on the size assigned to solvent molecules; see ref. 3 for the analytical expressions to calculate SASA). Specifically, the N-state is a sphere of radius  $a = 10 \text{ \AA}$ ,  $V_{\text{vdW}} = 4189 \text{ \AA}^3$  and SASA =  $1633 \text{ \AA}^2$  in  $\text{H}_2\text{O}$ , and  $2027 \text{ \AA}^2$  in  $\text{CCl}_4$  (calculated using for  $\text{H}_2\text{O}$  the  $1.4 \text{ \AA}$  radius, and for  $\text{CCl}_4$  the  $2.7 \text{ \AA}$  radius), whereas the D-state is a prolate spherocylinder of radius  $a = 4 \text{ \AA}$ , cylindrical length  $l = 78 \text{ \AA}$ ,  $V_{\text{vdW}} = 4189 \text{ \AA}^3$  and SASA =  $3013 \text{ \AA}^2$  in  $\text{H}_2\text{O}$ , and  $3848 \text{ \AA}^2$  in

CCl<sub>4</sub>; these numbers are reliable for a 50-residue globular protein. (2) The  $\Delta\Delta G_C$  contribution is estimated by calculating the reversible work to create in the different solvents the corresponding cavities, by assuming that each solvent can be treated as a hard sphere fluid possessing the experimental density of the actual liquid at the desired temperature. The classic SPT formula for a spherocylindrical cavity of radius  $a$  and cylindrical length  $l$  in a hard sphere fluid mixture,<sup>12</sup> derived by means of the geometric approach (the pressure-volume term is neglected for its smallness at  $P = 1$  atm) is:

$$\Delta G_C = RT \cdot \{-\ln(1-\xi_3) + [6\xi_2/(1-\xi_3)]a + [12\xi_1/(1-\xi_3)]a^2 + [18\xi_2^2/(1-\xi_3)^2]a^2 + [3\xi_2/2(1-\xi_3)]l + [6\xi_1/(1-\xi_3)]a \cdot l + [9\xi_2^2/(1-\xi_3)^2]a \cdot l\} \quad (12)$$

where  $\xi_i = (\pi/6) \cdot \sum \rho_j \cdot \sigma_j^i$ , and  $\rho_j$  is the number density, in molecules per  $\text{\AA}^3$ , of the species  $j$  and  $\sigma_j$  is the corresponding hard sphere diameter;  $\xi_3 = (\pi/6) \cdot \sum \rho_j \cdot \sigma_j^3$  represents the volume packing density of the hard sphere fluid mixture. By setting  $l = 0$ , the formula becomes right for a spherical cavity of radius  $a$ ; by considering only one component, eqn (12) corresponds to that for a hard sphere fluid. To perform classic SPT calculations over a large temperature range and 1 atm, the values of the experimental density of the different solvents have been used;<sup>14,26-28</sup> they are listed in the second column of Tables 1-4 (in some cases an extrapolation of experimental data has been performed to cover a larger temperature range; these values are marked with an asterisk). A critical point is the selection of the effective hard sphere diameter of the solvent molecules, assumed to be temperature-independent. I have selected:  $\sigma(\text{H}_2\text{O}) = 2.80 \text{ \AA}$ , which is close to the location of the first peak of the O-O radial distribution function of water,<sup>29</sup> and allows a satisfactory description of the cavity size distribution function of water;<sup>30</sup>  $\sigma(\text{MeOH}) = 3.83 \text{ \AA}$ , as determined by Ben-Amotz and Willis;<sup>31</sup>  $\sigma(\text{CCl}_4) = 5.37 \text{ \AA}$ , as determined by Wilhelm and Battino.<sup>32</sup> (3) The  $T \cdot \Delta S_{\text{conf}}$  term of eqn (11) can be calculated with the assumption that each residue gains an average, temperature-independent, conformational entropy upon denaturation/unfolding,<sup>3,4</sup> so that:

$$T \cdot \Delta S_{\text{conf}} = T \cdot N_{\text{res}} \cdot \Delta S_{\text{conf}}(\text{res}) \quad (13)$$

where  $N_{\text{res}} = 50$  and  $\Delta S_{\text{conf}}(\text{res}) = 24.4 \text{ J K}^{-1}\text{mol}\cdot\text{res}^{-1}$ ; the latter number is approximately in the middle of the range defined for globular proteins by the average value,  $14 \text{ J K}^{-1}\text{mol}\cdot\text{res}^{-1}$ , of the side chain entropy contribution, and the average value,  $40\text{-}50 \text{ J K}^{-1}\text{mol}\cdot\text{res}^{-1}$ , of the sum of backbone and side chain entropy contributions, on the basis of different theoretical and experimental determination procedures.<sup>33,34</sup> Recent NMR data and MD simulations have shown that the methyl groups of nonpolar side chains have a large rotational freedom in the folded state of globular proteins,<sup>35</sup> and so that the gain in conformational entropy upon denaturation should be smaller than that calculated in the past. The selected number tries to take into account these recent data. Note that, since globular proteins are heteropolymers, their conformational entropy should not be separated on a per residue contribution because backbone and side chain degrees of freedom are significantly coupled.<sup>36</sup>

## Results

**A. Water.** The SPT-calculated  $\Delta G_{\text{C}}(\text{N-state})$  and  $\Delta G_{\text{C}}(\text{D-state})$  functions in water are shown in Figure 1 over the  $-30$  to  $100 \text{ }^{\circ}\text{C}$  temperature range (the numbers are listed in the last two columns of Table 1). Both increase markedly with temperature and have a parabolic shape with a maximum above  $100 \text{ }^{\circ}\text{C}$ . Cavity creation proves to be significantly less costly on lowering the temperature below TMD for two reasons: (a) the water density decrease due to the greater tetrahedral order occurring below TMD; look at the values of the molar volume in the second column of Table 1; (b) the  $RT$  term in the classic SPT formula (and in the exact statistical mechanical expression<sup>11</sup> of  $\Delta G_{\text{C}} = -RT \cdot \ln p_0$ , where  $p_0$  is the probability of finding zero solvent molecules in the desired cavity region), related to the random thermal energy of solvent molecules bombarding the cavity surface, decreases on lowering the temperature. It is evident that  $\Delta G_{\text{C}}(\text{D-state})$  is markedly larger than  $\Delta G_{\text{C}}(\text{N-state})$ . This happens because the  $\Delta G_{\text{C}}$  magnitude increases on raising the cavity SASA, even though the cavity  $V_{\text{vdW}}$  does not change, as it has been shown by means of both classic SPT calculations,<sup>3,8</sup> and computer simulations in detailed water models.<sup>37</sup>

The  $\Delta\Delta G_{\text{C}} = \Delta G_{\text{C}}(\text{D-state}) - \Delta G_{\text{C}}(\text{N-state})$  function is shown in Figure 2 together with the straight line of the  $T \cdot \Delta S_{\text{conf}} = T \cdot N_{\text{res}} \cdot \Delta S_{\text{conf}}(\text{res})$  term, in which  $N_{\text{res}} = 50$  and

$\Delta S_{\text{conf}}(\text{res}) = 24.4 \text{ J K}^{-1}\text{mol}\cdot\text{res}^{-1}$  [look at eqn (13) above]. The two functions intersect each other at two temperatures, indicating the existence of two conformational transitions for the “model” protein [note that, even though the  $\Delta S_{\text{conf}}(\text{res})$  estimate would not be numerically exact, there will be always two intersection temperatures if the  $T\cdot\Delta S_{\text{conf}}$  term is linear or approximately linear]. By subtracting the  $T\cdot\Delta S_{\text{conf}}$  straight line from the  $\Delta\Delta G_{\text{C}}$  function, one obtains the thermodynamic stability curve,<sup>38</sup>  $\Delta G_{\text{d}}$  versus  $T$ , of the “model” protein in water, that is shown in Figure 3. Such thermodynamic stability curve shows  $T_{\text{d}}(\text{cold}) \approx -26 \text{ }^{\circ}\text{C}$ ,  $T_{\text{d}}(\text{hot}) \approx 49 \text{ }^{\circ}\text{C}$ ,  $T_{\text{max}} \approx 8 \text{ }^{\circ}\text{C}$  and  $\Delta G_{\text{d}}(T_{\text{max}}) \approx 10 \text{ kJ mol}^{-1}$ ; these numbers are reliable for a small globular protein. It has been experimentally determined over a large set of small globular proteins<sup>39</sup> that  $T_{\text{max}} = 285 \pm 19 \text{ K}$  and  $\Delta G_{\text{d}}(T_{\text{max}}) = 25 - 50 \text{ kJ mol}^{-1}$  (i.e., small globular proteins are marginally stable<sup>40</sup>). The results reported in Figures 1-3, obtained by keeping  $\sigma(\text{H}_2\text{O}) = 2.80 \text{ \AA}$  and temperature-independent, indicate that the water density decrease and the decrease in random thermal energy of water molecules bombarding the cavity surface are responsible of the decrease in the magnitude of the stabilizing  $\Delta\Delta G_{\text{C}}$  contribution that leads to cold denaturation. This implies that the basic mechanism of cold denaturation, originally proposed,<sup>3,4</sup> holds also by considering  $\sigma(\text{H}_2\text{O}) = 2.80 \text{ \AA}$  and temperature-independent. It is possible to further test its reliability.

The present theoretical approach has to be able to explain the fact that cold denaturation is a process characterized by a decrease in both enthalpy and entropy.<sup>1,2</sup> Since it has been assumed  $\Delta E_{\text{a}}(\text{H}_2\text{O}) \approx 0$  over the whole temperature range, the denaturation enthalpy change,  $\Delta H_{\text{d}}$ , has to be equal to the difference in the cavity enthalpy change,  $\Delta\Delta H_{\text{C}}$ , on passing from the N-state (i.e., the sphere) to the D-state (i.e., the prolate spherocylinder). The  $\Delta\Delta H_{\text{C}}$  numbers have been obtained by performing a numerical differentiation of the  $\Delta\Delta G_{\text{C}}$  function. It results that  $\Delta H_{\text{d}} = \Delta\Delta H_{\text{C}} \approx -145 \text{ kJ mol}^{-1}$  at  $T_{\text{d}}(\text{cold}) \approx -26 \text{ }^{\circ}\text{C}$ , and  $\Delta H_{\text{d}} = \Delta\Delta H_{\text{C}} \approx 130 \text{ kJ mol}^{-1}$  at  $T_{\text{d}}(\text{hot}) \approx 49 \text{ }^{\circ}\text{C}$ ; these numbers are reliable for a 50-residue protein. Cold denaturation proves to be exothermic and hot denaturation proves to be endothermic, as it is. Moreover, the change in heat capacity upon denaturation proves to be large and positive,  $\Delta C_{\text{p,d}} = (d\Delta\Delta H_{\text{C}}/dT) \approx 3.9 \text{ kJ K}^{-1}\text{mol}^{-1}$  at  $T_{\text{d}}(\text{cold})$ , and  $2.8 \text{ kJ K}^{-1}\text{mol}^{-1}$  at  $T_{\text{d}}(\text{hot})$ , in line with experimental data.<sup>1,2</sup> The  $\Delta H_{\text{C}}$  term accounts for the structural reorganization of solvent

molecules upon cavity creation.<sup>41</sup> According to Pierotti's application of classic SPT,<sup>42</sup> it is proportional to the isobaric thermal expansion coefficient  $\alpha_P$  of the solvent (see Appendix C). It is well known that  $\alpha_P$  of water shows a strong temperature dependence:<sup>14</sup>  $\alpha_P < 0$  for  $T < TMD$ ,  $\alpha_P = 0$  at  $T = TMD$  and  $\alpha_P > 0$  for  $T > TMD$  (see the numbers listed in the third column of Table 1). However, why is cavity creation exothermic below TMD and endothermic above TMD?

According to statistical mechanics,<sup>43</sup>  $\alpha_P = \langle (V - \langle V \rangle) \cdot (H - \langle H \rangle) \rangle / kT^2$ ; it is proportional to the ensemble correlation between volume fluctuations and enthalpy fluctuations (the latter in water are usually associated with transient H-bond reorganization). A positive correlation means that a positive volume fluctuation is associated with a positive enthalpy fluctuation: a volume increase leads to an enthalpy increase (i.e., a partial breaking of H-bonds in water). A negative correlation means that a positive volume fluctuation is associated with a negative enthalpy fluctuation: a volume increase leads to an enthalpy decrease (i.e., the H-bonded network is more ordered and more open because the H-bonds are more intact). Therefore, according to the present theoretical approach: (1) the structural reorganization of water molecules is more extensive around the D-state than around the N-state due to the larger SASA of the former state; (2) cold denaturation is exothermic because  $\alpha_P < 0$  for  $T < TMD$ , i.e., the structural reorganization of water molecules, upon unfolding, around the polypeptide chain leads to H-bonds less broken than those in bulk water; (3) hot denaturation is endothermic because  $\alpha_P > 0$  for  $T > TMD$ , i.e., the structural reorganization of water molecules, upon unfolding, around the polypeptide chain leads to H-bonds more broken than those in bulk water. However, it should be stressed that the exothermic H-bond contribution is not the cause of cold denaturation because it is exactly compensated by the entropy decrease associated with the same reorganization of water-water H-bonds<sup>20-22</sup> (a "reverse" sentence holds for hot denaturation). This enthalpy-entropy compensation is a fundamental feature of the structural reorganization of solvent molecules upon cavity creation.<sup>44</sup> Therefore, the formation of good clathrate cages around nonpolar moieties, detected in MD simulations around a cold-denatured small polymer in the so-called

Mercedes-Benz model of water,<sup>45</sup> is not in contrast with the present approach, but cannot be responsible for cold denaturation.<sup>46</sup>

A final point merits attention. The temperature where  $\Delta G_D$  is maximum corresponds to the temperature where the overall entropy change upon denaturation is zero. At  $T_{\max} \approx 8^\circ\text{C}$  there is perfect balance between the gain in conformational entropy of the polypeptide chain upon unfolding,  $\Delta S_{\text{conf}}$ , and the loss in entropy of water molecules due to the creation of the two different cavities,  $\Delta\Delta S_C$ . The latter, according to statistical mechanics, consists of two contributions:<sup>41,44</sup> (a) the loss in configurational/translational entropy of water molecules due to the SASA increase upon unfolding; (b) the gain/loss (depending on temperature) of entropy due to the structural reorganization of water-water H-bonds (this entropy contribution is compensated by the  $\Delta\Delta H_C$  term, as pointed out above; see also Appendix C). This is a subtle feature, but has to be recognized.

**B. Aqueous 40% (by weight) MeOH.** In order to verify whether the devised theoretical approach is able to distinguish between water and other solvents, the same calculation procedure has been applied to the same “model” protein in aqueous 40% (by weight) MeOH solution (the reasons for choosing such a solvent will become clear in the following). The SPT-calculated  $\Delta G_C(\text{N-state})$  and  $\Delta G_C(\text{D-state})$  functions are shown in Figure 4, and the numbers are listed in the last two columns of Table 2. These functions increase, more or less linearly over the  $-30$  to  $70^\circ\text{C}$  temperature range; their values, up to  $T < 10^\circ\text{C}$ , are larger than those calculated in water, and, for  $T > 10^\circ\text{C}$ , become smaller in magnitude than those calculated in water (compare the numbers listed in the last two columns of Tables 1 and 2). This important finding is a consequence of the fact that the density of aqueous 40% (by weight) MeOH always increases on lowering the temperature (see the numbers listed in the second column of Table 2), whereas the density of water decreases on lowering the temperature below TMD. For  $T > \text{TMD}$  the  $\Delta G_C$  values are larger in water than in 40% MeOH because: (a) the density of water decreases to a smaller extent than that of 40% MeOH due to the strength of the 3D H-bonded network; (b) water molecules are smaller in size than those of MeOH [i.e.,  $\sigma(\text{H}_2\text{O}) = 2.80 \text{ \AA}$  versus  $\sigma(\text{MeOH}) = 3.83 \text{ \AA}$ ], and so water proves to be characterized by a larger number density than 40% MeOH, even though the volume packing

density of the latter is larger<sup>6</sup> (i.e., look at the  $\xi_3$  values listed in the fifth columns of Tables 1 and 2).

As in the case of water,  $\Delta G_C(\text{D-state})$  is markedly larger than  $\Delta G_C(\text{N-state})$  because SASA(D-state) is larger than SASA(N-state), and SASA is a good measure of the solvent-excluded volume effect due to cavity creation.<sup>3,4,8</sup> The  $\Delta\Delta G_C = \Delta G_C(\text{D-state}) - \Delta G_C(\text{N-state})$  function, shown in Figure 5, increases almost linearly with temperature and intersects the  $T \cdot \Delta S_{\text{conf}}$  straight line (calculated using the same numbers as in water) at only one temperature. There is no evidence of cold denaturation. In particular,  $T_d(\text{hot}) \approx 20$  °C and  $\Delta H_d = \Delta\Delta H_C \approx 180$  kJ mol<sup>-1</sup> at this temperature. The “model” protein shows only the hot denaturation, at a low temperature, but the denaturation enthalpy change is larger than that in water if the two functions are compared at the same temperature (i.e., 180 versus 50 kJ mol<sup>-1</sup> at 20 °C). The latter finding is a consequence of the fact that  $\alpha_p$  in 40% MeOH is larger than in water at 20 °C:<sup>41,42</sup>  $0.63 \cdot 10^{-3}$  K<sup>-1</sup> versus  $0.21 \cdot 10^{-3}$  K<sup>-1</sup>. In addition, the  $\alpha_p$  values in 40% MeOH are around  $0.6 \cdot 10^{-3}$  K<sup>-1</sup> over the whole considered temperature range from -30 to 70 °C, in complete contrast with the behaviour in water (compare the numbers in the third column of Table 1 with those in the fourth column of Table 2). This implies that the structural reorganization upon cavity creation in 40% MeOH is totally different from that occurring in water. These results are in line with experimental data obtained by Woolfson and colleagues<sup>47</sup> on bovine ubiquitin (76 residues) by performing DSC measurements. At pH  $\approx$  2, they found: (a)  $T_d = 55$  °C,  $\Delta H_d(T_d) \approx 150$  kJ mol<sup>-1</sup> and  $\Delta C_{p,d} = 4.8$  kJ K<sup>-1</sup>mol<sup>-1</sup> in water; (b)  $T_d = 20$  °C,  $\Delta H_d(T_d) \approx 200$  kJ mol<sup>-1</sup> and  $\Delta C_{p,d} = 0$  in 40% MeOH; (c) the  $\Delta H_d(T_d)$  value depends strongly upon the solvent in which the protein is dissolved, and cannot be considered a right measure of protein stability. The NMR spectra reported by Woolfson and colleagues<sup>47</sup> show that: (a) bovine ubiquitin in 40% MeOH, at pH 2 and low temperature, populates the N-state identical to that existing in water; (b) it populates, upon temperature-induced unfolding, the so-called A-state (i.e., alcohol-state), a conformation possessing a lot of secondary structure elements but with nonpolar side chains entirely accessible to solvent (a recent NMR study<sup>48</sup> has shown that the cold denatured state of ubiquitin, at 258 K and 2500 atm, should resemble the A-state). According to the present theoretical approach, a globular

protein should be less stable in 40% MeOH than in water with respect to hot denaturation [i.e., lower  $T_d(\text{hot})$  value] because the stabilizing  $\Delta\Delta G_C$  contribution is smaller in magnitude for  $T > TMD$  of water. However, a globular protein should not undergo cold denaturation in 40% MeOH because the stabilizing  $\Delta\Delta G_C$  contribution does not decrease significantly on lowering the temperature, as a consequence of the density behaviour, rendering impossible the occurrence of cold denaturation according to the mechanism holding in water. Note, in this respect, that Privalov<sup>49</sup> stated that alcohols do not aid in the observation of cold denaturation.

**C. Methanol.** The SPT-calculated  $\Delta G_C(\text{N-state})$  and  $\Delta G_C(\text{D-state})$  functions in MeOH are shown in Figure 6, and the numbers are listed in the last two columns of Table 3. They present a very flat parabolic shape with a maximum around 50 °C and decrease at high temperatures. This happens because the density of MeOH decreases significantly, by 11.7%, over the 0 to 90 °C temperature range (see the numbers in the second column of Table 3), rendering less costly the process of cavity creation. The significant density decrease of MeOH contrasts with the water behaviour (its density decreases by 4.3% over the 0 to 100 °C temperature range) and is a consequence of the absence of a 3D H-bonded network in the former liquid. In addition, the  $\Delta G_C(\text{N-state})$  and  $\Delta G_C(\text{D-state})$  functions prove to be markedly smaller in magnitude than those calculated in both water and 40% MeOH. This happens because the size of MeOH molecules is larger than that of water molecules, as underscored above.<sup>6,7</sup> Also in this case  $\Delta G_C(\text{D-state})$  is markedly larger than  $\Delta G_C(\text{N-state})$  because  $SASA(\text{D-state})$  is larger than  $SASA(\text{N-state})$ . The  $\Delta\Delta G_C = \Delta G_C(\text{D-state}) - \Delta G_C(\text{N-state})$  function, shown in Figure 7, has a very flat parabolic shape and is smaller in magnitude than the  $T \cdot \Delta S_{\text{conf}}$  straight line (calculated using the same numbers as in water) over the whole considered temperature range. This means that the N-state is always less stable than the D-state, because the gain in configurational/translational entropy of MeOH molecules upon folding is always exceeded by the loss in conformational entropy of the polypeptide chain upon folding. Such a result is in line with well-established experimental data showing that the stability of the folded state of globular proteins strongly decreases on increasing the MeOH concentration in aqueous solution.<sup>50</sup>

**D. Carbon tetrachloride.** As a final test, the same type of calculations has been performed in  $\text{CCl}_4$ , a typical organic solvent with almost spherical molecules and no H-bonds. The SPT-calculated  $\Delta G_{\text{C}}(\text{N-state})$  and  $\Delta G_{\text{C}}(\text{D-state})$  functions in  $\text{CCl}_4$  are shown in Figure 8, and the numbers are listed in the last two columns of Table 4. They are practically constant up to 20 °C and then decrease in magnitude on further raising temperature. This temperature dependence originates from the significant decrease of  $\text{CCl}_4$  density with temperature as a consequence of the weakness of van der Waals interactions (see the molar volume values listed in the second column of Table 4). The SPT-calculated  $\Delta G_{\text{C}}(\text{N-state})$  and  $\Delta G_{\text{C}}(\text{D-state})$  functions in  $\text{CCl}_4$  prove to be markedly smaller than those calculated in the other three solvents, even though  $\text{CCl}_4$  has the largest volume packing density (compare the  $\xi_3$  values listed in the fifth column of Tables 1-4). This happens because  $\text{CCl}_4$  molecules are the largest:<sup>6,7</sup>  $\sigma(\text{CCl}_4) = 5.37 \text{ \AA}$ ,  $\sigma(\text{MeOH}) = 3.83 \text{ \AA}$  and  $\sigma(\text{H}_2\text{O}) = 2.80 \text{ \AA}$ . As a general result,  $\Delta G_{\text{C}}(\text{D-state})$  is markedly larger than  $\Delta G_{\text{C}}(\text{N-state})$ , because  $\text{SASA}(\text{D-state})$  is larger than  $\text{SASA}(\text{N-state})$ . The  $\Delta\Delta G_{\text{C}} = \Delta G_{\text{C}}(\text{D-state}) - \Delta G_{\text{C}}(\text{N-state})$  function, shown in Figure 9, has a very flat shape in  $\text{CCl}_4$  and is smaller in magnitude than the  $T \cdot \Delta S_{\text{conf}}$  straight line (calculated using the same numbers as in water) over the whole considered temperature range. This implies that the D-state is always more stable than the N-state, because the loss in conformational entropy of the polypeptide chain upon folding exceeds the gain in configurational/translational entropy of  $\text{CCl}_4$  molecules upon folding. This result seems to be in contrast with the experimental findings that the folded state of globular proteins is very stable in anhydrous nonpolar solvents.<sup>51</sup> However, one has to remember that the assumption  $\Delta E_{\text{a}} \approx 0$  should be reliable and correct in water, but it is expected to be wrong in a liquid such as  $\text{CCl}_4$ , whose molecules are not able to form H-bonds with peptide groups. So the  $\Delta E_{\text{a}}$  term can be positive and large in anhydrous nonpolar solvents, stabilizing the folded state of globular proteins.

## Discussion

The present results indicate that the devised theoretical approach and calculation procedure, notwithstanding the gross approximations, are able to account for the occurrence

of cold denaturation and its thermodynamic features in water, and for the marked difference existing between water and other liquids. Since the effective hard sphere diameter of solvent molecules is considered to be temperature-independent, the special temperature dependence of water density is fundamental in decreasing the magnitude of the stabilizing  $\Delta\Delta G_C$  term on lowering the temperature (together with the decrease in random thermal energy), determined by the special features of H-bonds. Furthermore, the small size of water molecules enlarges the magnitude of the solvent-excluded volume effect (i.e., the  $\Delta\Delta G_C$  term), and the N-state proves to be stable in a closed temperature range solely in water. The comparison performed between water, 40% (by weight) MeOH, MeOH and  $\text{CCl}_4$  clarifies unequivocally these points and strengthens the reliability of the proposed mechanism of cold denaturation.<sup>3</sup> An obvious criticism is that yeast frataxin<sup>2</sup> shows cold denaturation at 7 °C, a temperature slightly above TMD of water. Actually, the theoretical approach does not use TMD, but the experimental density values, producing a parabolic shape for the  $\Delta\Delta G_C$  term, and cold denaturation can happen above TMD depending on the intersection between the  $\Delta\Delta G_C$  curve and the  $T \cdot \Delta S_{\text{conf}}$  straight line. The devised model is able to rationalize other features of the conformational stability of globular proteins, such as the effects of cavity-creating point mutations (see Appendix D). Thus, it seems able to capture the fundamental ingredients of cold denaturation, providing insight into the molecular mechanisms governing the conformational stability of globular proteins, but sacrificing numerical accuracy. Note that it is completely different from the statistical mechanical models in which the parabola-like temperature dependence of the Gibbs energy change associated with the hydration of nonpolar groups is used as an input datum.<sup>52</sup>

Moreover, it has to be underscored that the revised SPT developed by Ashbaugh and Pratt<sup>53</sup> cannot rationalize in a straightforward manner the occurrence of cold denaturation. The  $\Delta G_C$  expression in this revised SPT depends on SASA through the experimental bulk liquid-vapour surface tension,  $\gamma_\infty$ , and its curvature dependence (the so-called Tolman length). The parabolic temperature dependence of  $\Delta G_C$  in water is not in line with the linear decrease of water  $\gamma_\infty$  on increasing temperature, and this leads to a marked temperature dependence of the Tolman length,<sup>53</sup> that passes from positive to negative values (i.e., a

strange result considering the geometric meaning of the Tolman length<sup>54</sup>). For cold denaturation, the marked decrease of  $\Delta G_C$  on lowering the temperature below TMD entirely contrasts with the corresponding increase in  $\gamma_\infty$ .

It is important to show that the present results are not in contrast with those obtained by Y&K;<sup>15</sup> the latter author provided a rationalization of cold denaturation, grounded on the role of the solvent-excluded volume effect, in another couple of articles.<sup>55</sup> They showed that cold denaturation is a manifestation of the basic fact that the magnitude of “hydrophobicity” (i.e., the solvent-excluded volume effect associated with cavity creation) becomes weaker on lowering the temperature. In particular, Y&K emphasized that water-water electrostatic interactions become stronger with respect to  $RT$  and play a dominant role, up to  $-15\text{ }^\circ\text{C}$ , with respect to the decrease in water number density. It is possible to cover a larger temperature range, by combining the Y&K results with the present ones, producing the following statement. On lowering the temperature below TMD, the water (number) density decreases because the water-water H-bonds become stronger, overwhelming the random thermal energy and producing a low-energy, tetrahedral network with a volume increase. So the strength of water-water H-bonds and their tetrahedral geometry play a major role.

In addition, eqn (6) of Y&K is practically identical to my eqn (11) and the  $\Delta\mu_{HS}$  quantity corresponds to the  $\Delta\Delta G_C$  term. They calculated  $\Delta\mu_{HS}$  for a protein modelled as a set of fused hard spheres in a realistic model of water and in a simple Lennard-Jones, LJ, solvent, having the same density of water at the respective temperature and whose particles have the same size of water molecules,  $\sigma(\text{H}_2\text{O}) = 2.80\text{ \AA}$ , assumed to be temperature-independent. Y&K found that, on passing from  $25\text{ }^\circ\text{C}$  to  $-15\text{ }^\circ\text{C}$ , the  $\Delta\mu_{HS}$  quantity decreases by  $115\text{ kJ mol}^{-1}$  in the water model, and by  $110\text{ kJ mol}^{-1}$  in the simple LJ solvent, suggesting the fundamental role played by the water density. However, cold denaturation occurs only in the water model because the magnitude of the  $\Delta\mu_{HS}$  quantity, at  $25\text{ }^\circ\text{C}$ , is markedly larger in the simple LJ solvent than in water,  $622$  versus  $479\text{ kJ mol}^{-1}$ . This result is not expected,<sup>56</sup> and was not explained by Y&K. It could be that  $\Delta\mu_{HS}$  is larger in the simple LJ solvent than in water because the former liquid is under high pressure to possess the same density of water,

and so the pressure-volume work proves to be large.<sup>57</sup> If this view were right, the results by Y&K would be in line with the present calculations and rationalization.

Moreover, Y&K<sup>15</sup> decomposed the hydration thermodynamic functions, such as  $\Delta\mu_{\text{HS}}$ , by means of the so-called morphometric approach,<sup>58</sup> that uses geometric properties of the solute molecule: its solvent-excluded volume, SEV, its SASA, and the SASA curvature. The SEV term is considered to account for the loss in translational entropy of bulk solvent molecules upon hydration, whereas the SASA term was considered to account for the loss in translational and orientational entropy upon hydration of the solvent molecules in contact with the solute surface<sup>15</sup> (i.e., the SEV term should be non-local in character, involving all the solvent molecules, whereas the SASA term should be local in character, involving only the solvent molecules in the first solvation shell). It is the SEV term that decreases on lowering the temperature (both in the water model and in the simple LJ solvent) and leads to cold denaturation. This result is only in apparent contrast with my approach and results because I have considered that the SEV decrease upon folding can be measured by the corresponding SASA decrease. Actually, the  $\Delta G_{\text{C}}$  quantity, that depends upon SEV, scales with SASA, as it has been shown by means of both classic SPT,<sup>41</sup> and detailed computer simulations in reliable liquid models.<sup>59</sup> Basically, this SASA dependence has to be connected with the explanation of the solvent-excluded volume effect provided in the Introduction section (see also the geometrical derivation<sup>12</sup> of the classic SPT formula for  $\Delta G_{\text{C}}$ ). The large numerical coefficient associated with the SEV term by Y&K is the consequence of the fundamental role played by the solvent-excluded volume effect in the hydration thermodynamics of molecular solutes (note that a globular protein is still a molecular solute and is not large enough to satisfy the large-solute limit). A final point has to be underscored. Y&K considered the thermodynamic quantities at constant volume, whereas the present approach considers those at constant pressure. This difference does not create problems, as spelled out in detail by Y&K.<sup>15</sup> Therefore, I think that the results by Y&K are in line with the present rationalization of the mechanism of cold denaturation.

In conclusion, by performing the same type of approximations and calculations in water, 40% (by weight) MeOH, MeOH, and  $\text{CCl}_4$ , the devised model shows that cold

denaturation occurs only in water due to the special temperature dependence of its density and due to the small size of its molecules. These two coupled factors determine the magnitude and the temperature dependence of the always stabilizing  $\Delta\Delta G_C$  term, that measures the gain in configurational/translational entropy of water molecules upon folding of the polypeptide chain.

## Appendix A: Conformational entropy change

The  $RT \cdot \ln(q_D/q_N)$  term in eqn (9) has been treated as the conformational entropy change associated with unfolding. A justification can be provided on the basis of the results obtained by Karplus and colleagues.<sup>60</sup> By assuming that the N-state corresponds to a single conformation, its conformational entropy should correspond to its vibrational entropy that comes from the accessibility of its normal modes (i.e., fluctuations in the neighbourhood of the N-state). In the case of the D-state ensemble, there are two contributions to the conformational entropy: first, the vibrational entropy associated with the accessibility of the normal modes of each unfolded conformation, and second, the entropy associated with the population distribution over the huge number of unfolded conformations. Karplus and colleagues showed that the vibrational entropy of the N-state is almost equal to the first entropy contribution of the D-state, given by the sum of the normal-mode entropies of unfolded conformations, each weighted by its fractional occupancy.<sup>58</sup> This finding implies that  $T \cdot \Delta S_{\text{conf}} \approx RT \cdot \ln(q_D/q_N)$ .

A further point emerged from the statistical mechanical derivation is that the obtained expression of the chemical potential does not allow the inclusion of the effects of the surroundings on the average structural features of the ensemble of native conformations and of the ensemble of denatured conformations. This is a consequence of the fact that the internal partition function  $q$ , is considered to be constant with respect to the surroundings and so not included in the configurational integral.<sup>16</sup> This procedure is correct for a simple molecule, but not for a polymer molecule that has an ensemble of accessible conformations. The right procedure should take into account that the potential energy of interaction of a polymer molecule with the surroundings depends upon the conformation of the polymer molecule itself. This right procedure, however, leads to a problem: the role of the solvent-excluded volume effect does not emerge in a simple manner.

**Appendix B: On the assumption  $\Delta E_a(\text{H}_2\text{O}) \approx 0$** 

In the interior of the folded state of globular proteins a lot of H-bonds and van der Waals contacts are turned on. Unfolding causes the disruption of most of these intra-protein interactions, but protein groups should be able to do the “same” attractive interactions with surrounding water molecules in unfolded conformations. An almost complete balance between the three energetic terms in the second square bracket of eqn (9) in the case of water should be a reliable approximation.<sup>3</sup> The assumption  $\Delta E_a(\text{H}_2\text{O}) \approx 0$  can also be a “strong” constraint to have a stable folded state. The inability to form in the interior of the folded state the “same” attractive interactions occurring with water molecules in unfolded conformations should cause a large energetic penalty that would render the folded state thermodynamically unstable. This should be the case of natively unfolded proteins.<sup>61</sup>

Moreover, by studying the swelling of a hydrophobic chain in TIP5P water by means of MD simulations,<sup>62</sup> it has been found that “the potential energy of the polymer changes by just 8.4 kJ mol<sup>-1</sup> which is due to the fact that the loss of intramolecular interactions when going from the collapsed to the swelled state is almost completely compensated by polymer/solvent interactions.” The results of MD simulations performed by Lazaridis and Karplus on the CI2 protein,<sup>63</sup> comparing the N-state and three compact denatured conformations, indicated that the enthalpy content is practically the same at 280 K and not so different at 320 K (see Table 2 in ref. 63). Notwithstanding the general warning that the results of MD simulations show a strong dependence on the force-field selected for the protein and the water model used,<sup>64</sup> these findings suggest that the energetic balance is operative and the assumption  $\Delta E_a(\text{H}_2\text{O}) \approx 0$  is not unreasonable.

Finally, it is worth noting that, even though the three energetic terms constituting  $\Delta E_a(\text{H}_2\text{O})$  would not cancel totally [see eqns (9) and (10)], the remainder should have only a small temperature dependence. The presence of this  $\Delta E_a(\text{H}_2\text{O})$  term will raise or lower the  $\Delta\Delta G_C$  curve in Figure 2 along the y-axis, causing a shift in the values of denaturation temperatures, but it will not modify the result that cold denaturation, in water, can happen by the proposed mechanism.

### Appendix C. Solvent reorganization upon cavity creation

Even though classic SPT is a hard sphere theory, the use of the experimental values of the density at the various temperatures in SPT formulae, allows one to take into account the role played by intermolecular interactions in each solvent<sup>41,42</sup> (H-bonds in water, for instance), also with respect to the structural reorganization of solvent molecules upon cavity creation. To clarify this important feature of the classic SPT treatment, it is convenient to consider the exact formula for the reversible work associated with the creation of a point cavity<sup>11</sup> (i.e., a cavity of radius  $a = 0$ ):

$$\Delta G_C(a = 0) = -RT \cdot \ln(1 - \xi_3) \quad (C1)$$

$\Delta G_C(a = 0)$  is a positive quantity because there is a solvent-excluded volume effect also for the creation of a point cavity: the spherical shell between the point cavity and its solvent accessible surface proves to be inaccessible to the centre of all solvent molecules because the cavity region has be void. The corresponding enthalpy and entropy changes are:

$$\Delta H_C(a = 0) = -T^2 \left\{ \frac{\partial [\Delta G_C(a = 0)/T]}{\partial T} \right\}_P = -[RT^2/(1 - \xi_3)] \cdot (\partial \xi_3 / \partial T)_P \quad (C2)$$

$$\Delta S_C(a = 0) = -[\partial \Delta G_C(a = 0) / \partial T]_P = R \cdot \ln(1 - \xi_3) - [RT/(1 - \xi_3)] \cdot (\partial \xi_3 / \partial T)_P \quad (C3)$$

Since a cavity has no attractive interactions with solvent molecules,  $\Delta H_C$  accounts solely for the solvent structural reorganization upon cavity creation, and proves to be proportional to the isobaric thermal expansion coefficient of the solvent [i.e.,  $(\partial \xi_3 / \partial T)_P = -\alpha_P \cdot \xi_3$ ]. The entropy change is made up of two contributions: the first term on the right-hand-side of eqn (C3) is the solvent-excluded volume contribution and is a negative quantity; the second term represents the solvent structural reorganization contribution and is exactly compensated by the cavity enthalpy change. Clearly, the heat capacity change proves to be proportional to the temperature derivative of  $\alpha_P$ .

Therefore, by using the experimental density for each liquid at  $P = 1$  atm, over a large temperature range, as originally done by Pierotti,<sup>42</sup> it is possible to calculate  $\Delta G_c$  and also  $\Delta H_c$  and  $\Delta S_c$ , taking into account the effect of the real interactions existing between the liquid molecules. For instance,  $\Delta H_c$ , being proportional to  $\alpha_p$ , accounts in water for the H-bond reorganization and its temperature-dependence.

## Appendix D: Cavity-creating point mutations

When Leu→Ala point mutations have been performed at buried positions, a destabilization of the folded state of the mutant has been recorded with respect to the folded state of wild-type. Matthews and co-workers<sup>65</sup> showed, by solving several X-ray structures, that such mutations lead to cavity-creation in the core of T4 lysozyme and the measured destabilization correlates with the cavity volume. Thus, destabilization was ascribed to the loss of van der Waals interactions in the protein core. In particular, for the L99A mutant, NMR measurements<sup>66</sup> showed that the protein region close to the cavity is dynamically disordered with respect to wild-type, and high-pressure crystallography<sup>67</sup> showed that the cavity can be filled by 2 water molecules at 2000 atm of hydrostatic pressure.

It is possible to explain such destabilization according to the present theoretical approach. The  $\Delta E_a$  term should not be really affected by a single Leu→Ala mutation because the Ala side chain with respect to the Leu side chain is involved in less interactions both in the protein interior of the N-state and with surrounding water molecules in the D-state [i.e., the loss in  $\Delta E(\text{intra})$  is counterbalanced by the loss in  $E_a(\text{D-state})$ ]. The  $T \cdot \Delta S_{\text{conf}}$  term should be affected because the Leu→Ala mutation causes a decrease in the number of allowed conformations for the side chain, and this should stabilize the N-state of the mutant with respect to wild-type. By using the estimates of the side chain conformational entropy collected by Doig and Sternberg,<sup>68</sup> one obtains  $T \cdot \Delta \Delta S_{\text{conf}} \approx 3 \text{ kJ mol}^{-1}$  at 300 K, stabilizing the N-state of the mutant. Finally, the  $\Delta \Delta G_c$  term is significantly affected by the Leu→Ala mutation because the SASA change leads to a significant Gibbs energy change. The difference  $\Delta G_c(\text{D-state}|\text{mutant}) - \Delta G_c(\text{D-state}|\text{wild-type}) \approx \Delta G_c(\text{methane}) - \Delta G_c(\text{isobutane})$ , and the latter amounts to: (a)  $-22 \text{ kJ mol}^{-1}$  at 25 °C, as calculated by means of classic SPT in water, by fixing  $\sigma(\text{H}_2\text{O}) = 2.8 \text{ \AA}$ ,  $\sigma(\text{CH}_4) = 3.7 \text{ \AA}$ , and  $\sigma(\text{i-C}_4\text{H}_{10}) = 5.5 \text{ \AA}$ ; (b)  $-23 \text{ kJ mol}^{-1}$  at 25 °C in the SPC water model.<sup>69</sup> This quantity should correspond to the largest possible destabilization occurring when the overall structure of the N-state does not change and  $\Delta G_c(\text{N-state}|\text{mutant}) = \Delta G_c(\text{N-state}|\text{wild-type})$ . However, when the protein matrix reorganizes closing in part or totally the cavity,  $\Delta G_c(\text{N-state}|\text{mutant}) < \Delta G_c(\text{N-state}|\text{wild-type})$  and the destabilization can be smaller. The measured  $-\Delta \Delta G_D$  values fall in the range 9 –

22 kJ mol<sup>-1</sup> at 25 °C,<sup>65</sup> indicating that the devised theoretical approach is able to rationalize the effect of cavity-creating point mutations without the introduction of *ad hoc* assumptions. Lee<sup>70</sup> devised a different route to explain such experimental data, but the conclusions were similar to the present ones.

## References

1. P.L. Privalov, Y.V. Griko, S.Y. Venyaminov and V.P. Kutysenko, *J.Mol.Biol.*, 1986, **190**, 487-498; Y.V. Griko and P.L. Privalov, *Biochemistry*, 1992, **31**, 8810-8815; G.S. Buchner, N. Shih, A.E. Reece, S. Niebling and J. Kubelka, *Biochemistry*, 2012, **51**, 6496-6498; B. Luan, B. Shan, C. Baiz, A. Tokmakoff and D.P. Raleigh, *Biochemistry*, 2013, **52**, 2402-2409.
2. A. Pastore, S.R. Martin, A. Politou, K.C. Kondapalli, T. Stemmler and P.A. Temussi, *J.Am.Chem.Soc.*, 2007, **129**, 5374-5375; S.R. Martin, V. Esposito, P. De Los Rios, A. Pastore and P.A. Temussi, *J.Am.Chem.Soc.*, 2008, **130**, 9963-9970; M. Aznauryan, D. Nettels, A. Holla, H. Hofman and B. Schuler, *J.Am.Chem.Soc.*, 2013, **135**, 14040-14043; D. Bonetti, A. Toto, R. Giri, A. Morrone, D. Sanfelice, A. Pastore, P.A. Temussi, S. Gianni and M. Brunori, *Phys.Chem.Chem.Phys.*, 2014, **16**, 6391-6397.
3. G. Graziano, *Phys.Chem.Chem.Phys.*, 2010, **12**, 14245-14252.
4. A. Riccio and G. Graziano, *Proteins*, 2011, **79**, 1739-1746; G. Graziano, *Phys.Chem.Chem.Phys.*, 2012, **14**, 2769-2773.
5. B. Lee and F.M. Richards, *J.Mol.Biol.*, 1971, **55**, 379-400.
6. B. Lee, *Biopolymers*, 1985, **24**, 813-823; G. Graziano, *J.Phys.Chem.B*, 2002, **106**, 7713-7716; G. Graziano, *J.Chem.Phys.*, 2008, **109**, 084506.
7. The magnitude of this entropy loss increases: (a) on raising the volume packing density of the liquid, by keeping fixed the size of liquid molecules, because the fraction of void space decreases; (b) on decreasing the size of liquid molecules, by keeping fixed the volume packing density of the liquid, because the void space is partitioned in smaller pieces.
8. G. Graziano, *J.Phys.Chem.B*, 2009, **113**, 11232-11239; G. Graziano, *Chem.Phys.Lett.*, 2010, **499**, 79-82.
9. S. Miller, J. Janin, A.M. Lesk and C. Chothia, *J.Mol.Biol.*, 1987, **196**, 641-656; V.Z. Spassov, A.D. Karshikoff and R. Ladenstein, *Protein Sci.*, 1995, **4**, 1516-1527.
10. W. Kauzmann, *Adv.Protein Chem.*, 1959, **14**, 1-63.

11. J.L. Lebowitz, E. Helfand and E. Praestgaard, *J.Chem.Phys.*, 1965, **43**, 774-779; H. Reiss, *Adv.Chem.Phys.*, 1966, **9**, 1-84.
12. H. Reiss, *J.Phys.Chem.*, 1992, **92**, 4736-4747; G. Graziano, *Chem.Phys.Lett.*, 2007, **440**, 221-223.
13. G. Graziano, *Phys.Chem.Chem.Phys.*, 2011, **13**, 12008-12014; G. Graziano, *Phys.Chem.Chem.Phys.*, 2011, **13**, 17689-17695; G. Graziano, *Phys.Chem.Chem.Phys.*, 2012, **14**, 13088-13094; G. Graziano, *Chem.Phys.Lett.*, 2013, **556**, 292-296.
14. G.S. Kell, *J.Chem.Eng.Data*, 1975, **20**, 97-105.
15. T. Yoshidome and M. Kinoshita, *Phys.Chem.Chem.Phys.*, 2012, **14**, 14554-14566.
16. A. Ben-Naim, *Hydrophobic Interactions*, Plenum Press, New York, 1980.
17. A. Ben-Naim, *Solvation Thermodynamics*, Plenum Press, New York, 1987.
18. B. Widom, *J.Phys.Chem.*, 1982, **86**, 869-872.
19. B. Lee, *Biopolymers*, 1991, **31**, 993-1008; G. Graziano, *Chem.Phys.Lett.*, 2006, **429**, 114-118.
20. A. Ben-Naim, *Biopolymers*, 1975, **14**, 1337-1355; H.A. Yu and M.J. Karplus, *J.Chem.Phys.*, 1988, **89**, 2366-2379; E. Grunwald and C. Steel, *J.Am.Chem.Soc.*, 1995, **117**, 5687-5692; H. Qian and J.J. Hopfield, *J.Chem.Phys.*, 1996, **105**, 9292-9298.
21. B. Lee, *Biophys.Chem.*, 1994, **51**, 271-278; G. Graziano and B. Lee, *J.Phys.Chem.B*, 2001, **105**, 10367-10372.
22. Enthalpy-entropy compensation could not hold for the water-water H-bond reorganization around polar and charged solutes because the water molecules in the hydration shell make direct H-bonds with the solute molecule. Such direct solute-water H-bonds have to be correctly accounted for in the partitioning of the total enthalpy change. Assigning half of their energy to the water-water H-bond reorganization, enthalpy-entropy compensation proved to hold for the water-water H-bond reorganization associated with the hydration of *n*-alcohols [G. Graziano, *Phys.Chem.Chem.Phys.*, 1999, **1**, 3567-3576], and of *N*-methyl-acetamide [G.

- Graziano, *J.Phys.Soc.Jpn.*, 2000, **69**, 3720-3725]. This does not detract from the importance of characterizing the protein-water interactions via NMR measurements [N.V. Nucci, M.S. Pometum and A.J. Wand, *Nat.Struct.Mol.Biol.*, 2011, **18**, 245-249].
23. The use of eqn (11) allowed a more-than-qualitative rationalization of the Gibbs energy changes associated with the unfolding + extension of collapsed conformations of single hydrophobic chains in water [G. Graziano, *Phys.Chem.Chem.Phys.*, 2013, **15**, 7389-7395], determined over a large temperature range by means of atomic force microscopy measurements [I.T.S. Li and G.C. Walker, *Proc.Natl.Acad.Sci.U.S.A.*, 2011, **108**, 16527-16532].
24. G.N. Ramachandran, C. Ramakrishnan and V. Sasisekharan, *J.Mol.Biol.*, 1963, **7**, 95-99; A.Q. Zhou, C.S. O'Hern and L. Regan, *Protein Sci.*, 2011, **20**, 1166-1171.
25. The N-state and the D-state of a globular protein do not have exactly the same  $V_{vdW}$ . Richards [F.M. Richards, *Annu.Rev.Biophys.Bioeng.*, 1977, **6**, 151-176] defined the  $V_{vdW}$  for the protein states as the volume that is not accessible to any part of the spherical probe which is rolled over the surface of the protein. On this basis,  $V_{vdW}(N\text{-state}) > V_{vdW}(D\text{-state})$  because the intrinsic voids present inside the folded state are lost upon unfolding. However, the change in partial molar volume upon denaturation/unfolding, even though negative, is a very small quantity, leading to the so-called protein volume paradox [C.A. Royer, *Biochim.Biophys.Acta*, 2002, **1595**, 201-209; T.V. Chalikian, *Annu.Rev.Biophys.Biomol.Struct.*, 2003, **32**, 207-235]. The present analysis refers to  $P = 1$  atm and it should be safe to neglect the pressure-volume contribution to  $\Delta\Delta G_C$  due to its negligible magnitude (i.e.,  $P \cdot \Delta V_d \approx 0$ , if  $P = 1$  atm).
26. Technical Information & Safe Handling Guide for Methanol at [www.methanol.org](http://www.methanol.org).
27. R.D. Goodwin, *J.Phys.Chem.Ref.Data*, 1987, **16**, 799-892.
28. I. Cibulka, T. Takagi and K. Ruzika, *J.Chem.Eng.Data*, 2001, **46**, 2-28.
29. J.M. Sorenson, G. Hura, R.M. Glaeser and T. Head-Gordon, *J.Chem.Phys.*, 2000, **113**, 9149-9161.

30. A. Pohorille and L.R. Pratt, *J.Am.Chem.Soc.*, 1990, **112**, 5066-5074; G. Graziano, *Biophys.Chem.*, 2003, **104**, 393-405; G. Graziano, *Chem.Phys.Lett.*, 2004, **396**, 226-231.
31. D. Ben-Amotz and K.G. Willis, *J.Phys.Chem.*, 1993, **97**, 7736-7742.
32. E. Wilhelm and R. Battino, *J.Chem.Phys.*, 1971, **55**, 4012-4017.
33. T.P. Creamer and G.D. Rose, *Proc.Natl.Acad.Sci.U.S.A.*, 1992, **89**, 5937-5941; S.D. Pickett and M.J.E. Sternberg, *J.Mol.Biol.*, 1993, **231**, 825-839; J. Fitter, *Biophys.J.*, 2003, **84**, 3924-3930.
34. B. Honig and A.S. Yang, *Adv.Protein Chem.*, 1995, **46**, 27-58; G.I. Makhatadze and P.L. Privalov, *Adv.Protein Chem.*, 1995, **47**, 307-425; P.L. Privalov, *Pure Appl.Chem.*, 2007, **79**, 1445-1462.
35. V. Kasinath, K.A. Sharp and A.J. Wand, *J.Am.Chem.Soc.*, 2013, **135**, 15092-15100.
36. S. Bromberg and K.A. Dill, *Protein Sci.*, 1994, **3**, 997-1009; K.A. Dill and D. Stigter, *Adv.Protein Chem.*, 1995, **46**, 59-104.
37. A. Wallqvist and B.J. Berne, *J.Phys.Chem.*, 1995, **99**, 2885-2892; A.J. Patel, P. Varilly and D. Chandler, *J.Phys.Chem.B*, 2010, **114**, 1632-1637.
38. W.J. Becktel and J.A. Schellman, *Biopolymers*, 1987, **26**, 1859-1877.
39. D.C. Rees and A.D. Robertson, *Protein Sci.*, 2001, **10**, 1187-1194.
40. P.L. Privalov, *Adv.Protein Chem.*, 1979, **33**, 167-241.
41. G. Graziano, *J.Phys.Chem.B*, 2006, **110**, 11421-11426.
42. R.A. Pierotti, *Chem.Rev.*, 1976, **76**, 717-726.
43. T.L. Hill, *An Introduction to Statistical Thermodynamics*, Addison-Wesley, Reading, 1960.
44. B. Lee, *J.Chem.Phys.*, 1985, **83**, 2421-2425; G. Graziano, *J.Phys.Soc.Jpn.*, 2000, **69**, 1566-1569; G. Graziano, *J.Chem.Phys.*, 2004, **120**, 4467-4471.
45. C.L. Dias, T. Ala-Nissila, M. Karttunen, I. Vattulainen and M Grant, *Phys.Rev.Lett.*, 2008, **100**, 118101; C.L. Dias, *Phys.Rev.Lett.*, 2012, **109**, 048104.
46. G. Graziano, *Cryobiology*, 2010, **60**, 354-355.

47. D.N. Woolfson, A. Cooper, M.M. Harding, D.H. Williams and P.A. Evans, *J.Mol.Biol.*, 1993, **229**, 502-511.
48. N. Vajpai, L. Nisius, M. Wiktor and S. Grzesiek, *Proc.Natl.Acad.Sci.U.S.A.*, 2013, **110**, E368-E376.
49. P.L. Privalov, *Crit.Rev.Biochem.Mol.Biol.*, 1990, **25**, 281-305.
50. A.L. Fink and B. Painter, *Biochemistry*, 1987, **26**, 1665-1671.
51. A.M. Klibanov, *Nature*, 2001, **409**, 241-246; C.N. Pace, S. Trevino, E. Prabhakaran and J.M. Scholtz, *Phil.Trans.R.Soc.Lond.B*, 2004, **359**, 1225-1235.
52. K.A. Dill, D.O.V. Alonso and K. Hutchinson, *Biochemistry*, 1989, **28**, 5439-5449; J.K. Cheung, P.Shah and T.M. Truskett, *Biophys.J.*, 2006, **91**, 2427-2435; E. Ascolese and G. Graziano, *Chem.Phys.Lett.*, 2008, **467**, 150-153; A. Riccio, E. Ascolese and G. Graziano, *Chem.Phys.Lett.*, 2010, **486**, 65-69.
53. H.S. Ashbaugh and L.R. Pratt, *Rev.Mod.Phys.*, 2006, **78**, 159-178; H.S. Ashbaugh and L.R. Pratt, *J.Phys.Chem.B*, 2007, **111**, 9330-9336.
54. G. Graziano, *Chem.Phys.Lett.*, 2010, **497**, 33-36.
55. T. Yoshidome and M. Kinoshita, *Phys.Rev.E*, 2009, **79**, 030905; H. Oshima, T. Yoshidome, K. Amano and M. Kinoshita, *J.Chem.Phys.*, 2009, **131**, 205102; M. Kinoshita, *Int.J.Mol.Sci.*, 2009, **10**, 1064-1080.
56. L.R. Pratt and A. Pohorille, *Proc.Natl.Acad.Sci.U.S.A.*, 1992, **89**, 2995-2999.
57. G. Graziano, *J.Chem.Phys.*, 2014, **140**, 094503.
58. P.M. König, R. Roth and K.R. Mecke, *Phys.Rev.Lett.*, 2004, **93**, 160601.
59. K. Lum, D. Chandler and J.D. Weeks, *J.Phys.Chem.B*, 1999, **103**, 4570-4577; D. Chandler, *Nature*, 2005, **437**, 640-647; H.S. Ashbaugh and L.R. Pratt, *Rev.Mod.Phys.*, 2006, **78**, 159-178; H.S. Ashbaugh and L.R. Pratt, *J.Phys.Chem.B*, 2007, **111**, 9330-9336; R.C. Remsing and J.D. Weeks, *J.Phys.Chem.B*, 2013, **117**, 15479-15491.
60. M. Karplus, T. Ichiye and B.M. Pettitt, *Biophys.J.*, 1987, **52**, 1083-1085.
61. V.N. Uversky, *Protein Sci.*, 2002, **11**, 739-756.
62. D. Paschek, S. Nonn and A. Geiger, *Phys.Chem.Chem.Phys.*, 2005, **7**, 2780-2786.
63. T. Lazaridis and M. Karplus, *Biophys.Chem.*, 1999, **78**, 207-217.

64. D. Paschek, R. Day and A.E. Garcia, *Phys.Chem.Chem.Phys.*, 2011, **13**, 19840-19847.
65. A.E. Eriksson, W.A. Baase, X.J. Zhang, D.W. Heinz, M. Blaber, E.P. Baldwin and B.W. Matthews, *Science*, 1992, **255**, 178-183.
66. F.A.A. Mulder, B. Hon, A. Mittermaier, F.W. Dahlquist and L.E. Kay, *J.Am.Chem.Soc.*, 2002, **124**, 1443-1451.
67. M.D. Collins, G. Hummer, M.L. Quillin, B.W. Matthews and S.M. Gruner, *Proc.Natl.Acad.Sci.U.S.A.*, 2005, **102**, 16668-16671.
68. A.J. Doig and M.J.E. Sternberg, *Protein Sci.*, 1995, **4**, 2247-2251.
69. D. Trzesniak, N.F.A. van der Vegt and W.F. van Gunsteren, *Phys.Chem.Chem.Phys.*, 2004, **6**, 697-702.
70. B.Lee, *Protein Sci.*, 1993, **2**, 733-738.

**Table 1.** Experimental values for water of the molar volume, isobaric thermal expansion coefficient and isothermal compressibility over the -30 to 100 °C temperature range at 1 atm.<sup>14</sup> The values of the volume packing density and of the SPT-calculated  $\Delta G_C(\text{N-state})$  and  $\Delta G_C(\text{D-state})$  functions are listed in the last three columns.

T °C	$v$ cm <sup>3</sup> mol <sup>-1</sup>	$\alpha_P \cdot 10^3$ K <sup>-1</sup>	$\beta_T \cdot 10^{12}$ cm <sup>2</sup> dyne <sup>-1</sup>	$\xi_3$	$\Delta G_C(\text{N})$ kJ mol <sup>-1</sup>	$\Delta G_C(\text{D})$ kJ mol <sup>-1</sup>
-30	18.316	-1.40	80.8	0.378	386.5	680.7
-20	18.137	-0.661	64.3	0.382	411.6	724.8
-10	18.054	-0.292	55.8	0.383	432.6	761.7
0	18.023	-0.068	50.9	0.384	450.7	793.6
5	18.021	0.016	49.2	0.384	459.3	808.6
20	18.052	0.207	45.9	0.383	482.0	848.6
40	18.161	0.385	44.2	0.381	507.6	893.9
60	18.328	0.523	44.5	0.378	528.9	931.5
80	18.543	0.641	46.1	0.373	545.7	961.3
100	18.803	0.750	49.0	0.368	558.5	983.9

**Table 2.** Experimental values for aqueous 40% (by weight) MeOH solution of the density, isobaric thermal expansion coefficient and MeOH molarity over the -30 to 70 °C temperature range at 1 atm.<sup>26</sup> The values of the volume packing density and of the SPT-calculated  $\Delta G_c(\text{N-state})$  and  $\Delta G_c(\text{D-state})$  functions are listed in the last three columns. The asterisk indicates that the density value has been obtained by extrapolation.

T °C	d g l <sup>-1</sup>	$\alpha_p \cdot 10^3$ K <sup>-1</sup>	[MeOH] mol l <sup>-1</sup>	$\xi_3$	$\Delta G_c(\text{N})$ kJ mol <sup>-1</sup>	$\Delta G_c(\text{D})$ kJ mol <sup>-1</sup>
-30	964	0.61	12.1	0.436	423.4	745.8
-20	958	0.62	12.0	0.433	433.3	763.3
-10	952	0.62	11.9	0.430	442.8	780.0
0	947	0.62	11.8	0.428	453.3	798.6
10	941	0.63	11.8	0.425	462.1	814.3
20	935	0.63	11.7	0.423	471.6	831.1
30	928	0.64	11.6	0.419	477.4	841.5
50	917*	0.64	11.5	0.414	493.7	870.3
70	905*	0.65	11.3	0.409	507.8	895.5

**Table 3.** Experimental values for MeOH of the molar volume, isobaric thermal expansion coefficient and isothermal compressibility over the -30 to 90 °C temperature range at 1 atm.<sup>26,27</sup> The values of the volume packing density and of the SPT-calculated  $\Delta G_C(\text{N-state})$  and  $\Delta G_C(\text{D-state})$  functions are listed in the last three columns.

T °C	$v$ cm <sup>3</sup> mol <sup>-1</sup>	$\alpha_P \cdot 10^3$ K <sup>-1</sup>	$\beta_T \cdot 10^{12}$ cm <sup>2</sup> dyne <sup>-1</sup>	$\xi_3$	$\Delta G_C(\text{N})$ kJ mol <sup>-1</sup>	$\Delta G_C(\text{D})$ kJ mol <sup>-1</sup>
-30	38.26	1.10	94.3	0.463	355.6	627.8
-20	38.60	1.12	98.8	0.459	361.0	637.7
-10	39.04	1.14	103.7	0.454	363.8	642.7
0	39.51	1.16	109.2	0.448	365.4	645.8
20	40.43	1.19	122.0	0.438	368.6	651.8
40	41.41	1.23	138.3	0.428	369.8	654.1
60	42.46	1.27	159.5	0.417	368.9	653.1
80	43.55	1.30	182.4	0.407	367.2	650.4
90	44.13	1.32	195.4	0.401	365.5	647.5

**Table 4.** Experimental values for  $\text{CCl}_4$  of the molar volume, isobaric thermal expansion coefficient and isothermal compressibility over the -30 to 100 °C temperature range at 1 atm.<sup>28</sup> The values of the volume packing density and of the SPT-calculated  $\Delta G_{\text{C}}(\text{N-state})$  and  $\Delta G_{\text{C}}(\text{D-state})$  functions are listed in the last three columns.

T °C	$v$ $\text{cm}^3 \text{ mol}^{-1}$	$\alpha_{\text{P}} \cdot 10^3$ $\text{K}^{-1}$	$\beta_{\text{T}} \cdot 10^{12}$ $\text{cm}^2 \text{ dyne}^{-1}$	$\xi_3$	$\Delta G_{\text{C}}(\text{N})$ $\text{kJ mol}^{-1}$	$\Delta G_{\text{C}}(\text{D})$ $\text{kJ mol}^{-1}$
-30	91.03	1.08	68.1	0.536	293.9	520.9
-20	92.12	1.10	74.2	0.530	293.9	521.1
-10	93.21	1.12	80.7	0.524	293.9	521.2
0	94.27	1.14	87.7	0.518	294.2	522.0
20	96.49	1.19	103.2	0.506	293.1	520.5
40	98.88	1.25	121.3	0.494	290.5	516.2
60	101.46	1.32	142.8	0.481	286.2	509.0
80	104.26	1.40	169.5	0.468	280.5	499.4
100	107.32	1.49	204.4	0.455	273.6	487.4

## Captions to the Figures

**Figure 1.** Temperature dependence of the  $\Delta G_C$  functions calculated in water for the spherical cavity corresponding to the N-state, and the spherocylindrical cavity corresponding to the D-state.

**Figure 2.** The curve  $\Delta\Delta G_C = \Delta G_C(\text{D-state}) - \Delta G_C(\text{N-state})$  of Figure 1 (water) is shown with the  $T \cdot \Delta S_{\text{conf}}$  straight line, calculated fixing  $N_{\text{res}} = 50$  and  $\Delta S_{\text{conf}}(\text{res}) = 24.4 \text{ J K}^{-1} \text{ mol} \cdot \text{res}^{-1}$ .

**Figure 3.** Thermodynamic stability curve of the “model” globular protein in water, obtained by subtracting the  $T \cdot \Delta S_{\text{conf}}$  straight line to the  $\Delta\Delta G_C$  curve, both reported in Figure 2. It shows both the cold denaturation temperature and the hot denaturation one.

**Figure 4.** Temperature dependence of the  $\Delta G_C$  functions calculated in the aqueous 40% (by weight) MeOH solution for the spherical cavity corresponding to the N-state, and the spherocylindrical cavity corresponding to the D-state.

**Figure 5.** The curve  $\Delta\Delta G_C = \Delta G_C(\text{D-state}) - \Delta G_C(\text{N-state})$  of Figure 4 (40% MeOH in water) is shown together with the  $T \cdot \Delta S_{\text{conf}}$  straight line, calculated fixing  $N_{\text{res}} = 50$  and  $\Delta S_{\text{conf}}(\text{res}) = 24.4 \text{ J K}^{-1} \text{ mol} \cdot \text{res}^{-1}$ .

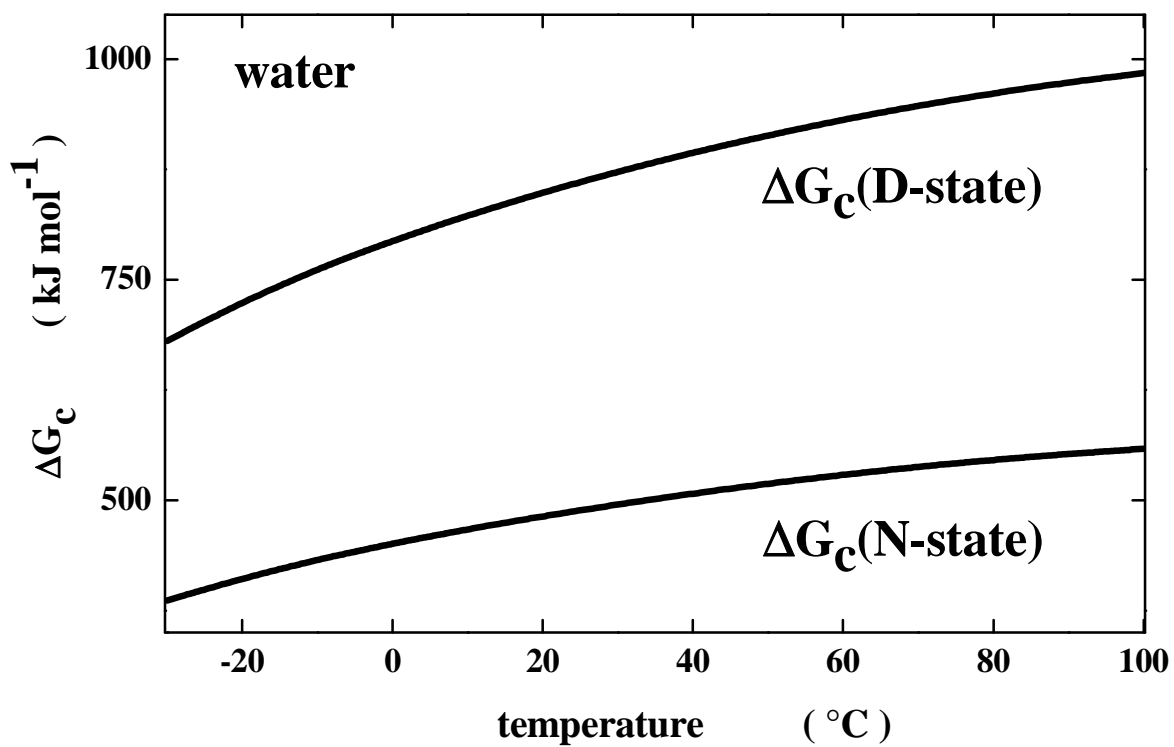
**Figure 6.** Temperature dependence of the  $\Delta G_C$  functions calculated in methanol for the spherical cavity corresponding to the N-state, and the spherocylindrical cavity corresponding to the D-state.

**Figure 7.** The curve  $\Delta\Delta G_C = \Delta G_C(\text{D-state}) - \Delta G_C(\text{N-state})$  of Figure 6 (methanol) is shown with the  $T \cdot \Delta S_{\text{conf}}$  line, calculated fixing  $N_{\text{res}} = 50$  and  $\Delta S_{\text{conf}}(\text{res}) = 24.4 \text{ J K}^{-1} \text{ mol} \cdot \text{res}^{-1}$ .

**Figure 8.** Temperature dependence of the  $\Delta G_C$  functions calculated in carbon tetrachloride for the spherical cavity corresponding to the N-state, and the spherocylindrical cavity corresponding to the D-state.

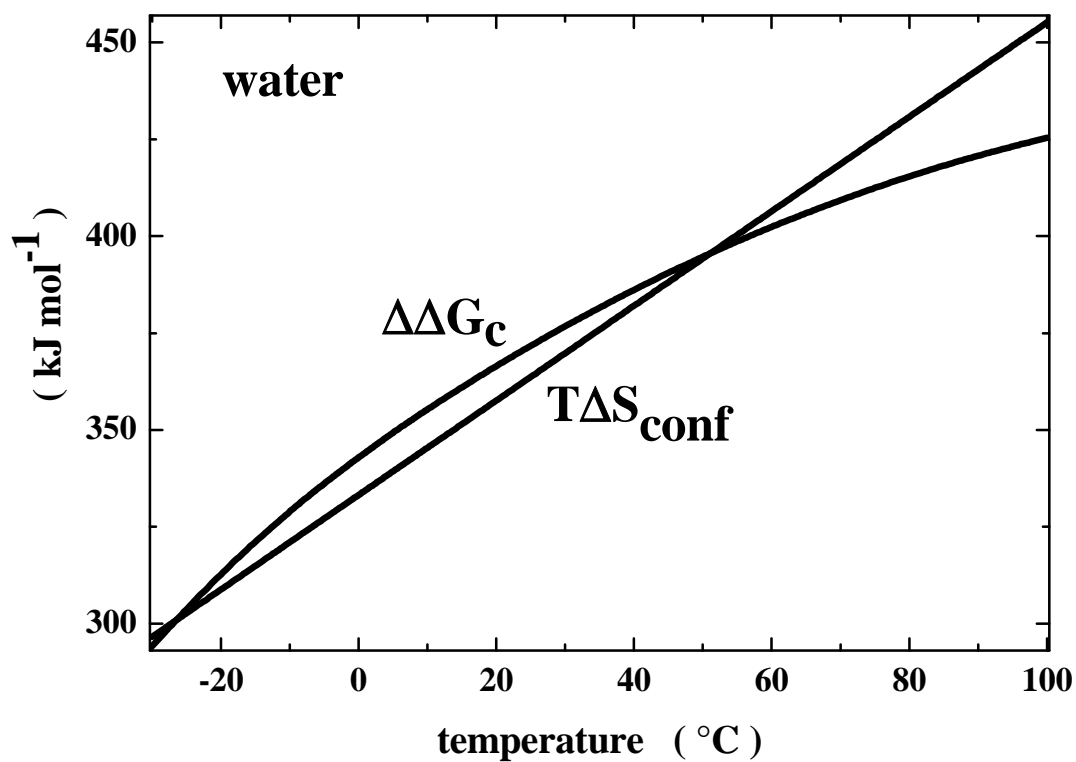
**Figure 9.** The curve  $\Delta\Delta G_C = \Delta G_C(\text{D-state}) - \Delta G_C(\text{N-state})$  of Figure 8 (carbon tetrachloride) is shown together with the  $T \cdot \Delta S_{\text{conf}}$  straight line, calculated fixing  $N_{\text{res}} = 50$  and  $\Delta S_{\text{conf}}(\text{res}) = 24.4 \text{ J K}^{-1} \text{ mol} \cdot \text{res}^{-1}$ .

Figure 1.



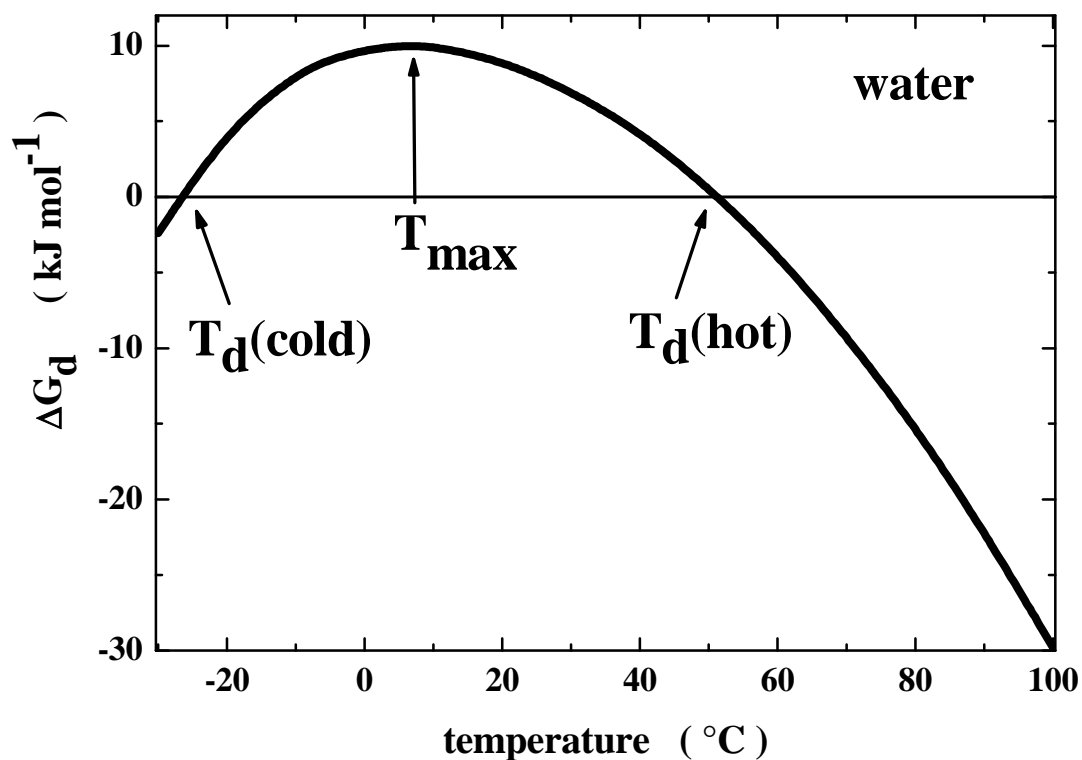
**Figure 1.** Temperature dependence of the  $\Delta G_c$  functions calculated in water for the spherical cavity corresponding to the N-state, and the spherocylindrical cavity corresponding to the D-state.

Figure 2.



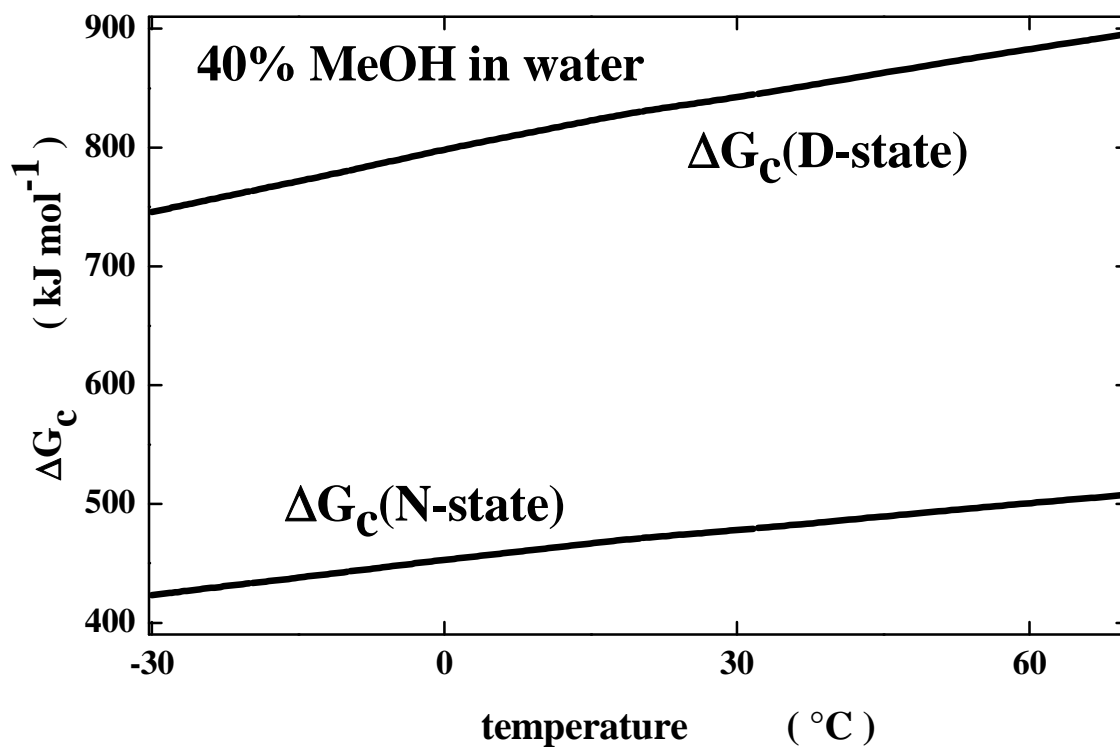
**Figure 2.** The curve  $\Delta\Delta G_c = \Delta G_c(\text{D-state}) - \Delta G_c(\text{N-state})$  of Figure 1 (water) is shown with the  $T\cdot\Delta S_{\text{conf}}$  straight line, calculated fixing  $N_{\text{res}} = 50$  and  $\Delta S_{\text{conf}}(\text{res}) = 24.4 \text{ J K}^{-1}\text{mol}\cdot\text{res}^{-1}$ .

Figure 3.



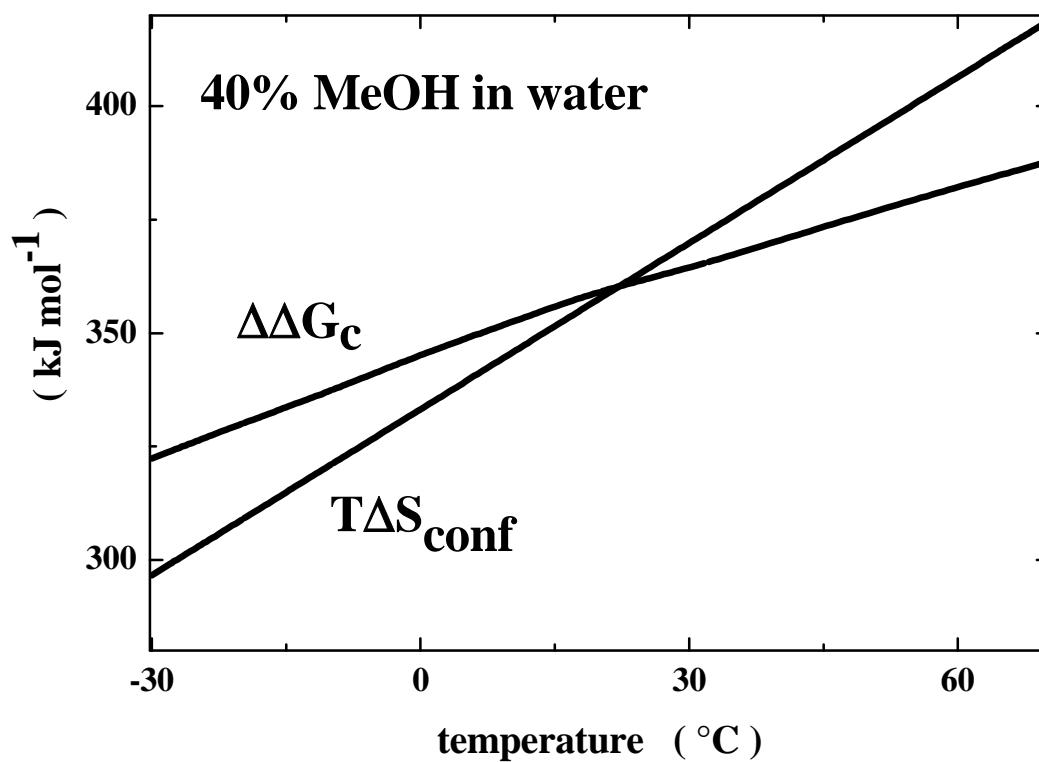
**Figure 3.** Thermodynamic stability curve of the “model” globular protein in water, obtained by subtracting the  $T \cdot \Delta S_{\text{conf}}$  straight line to the  $\Delta \Delta G_c$  curve, both reported in Figure 2. It shows both the cold denaturation temperature and the hot denaturation one.

Figure 4.



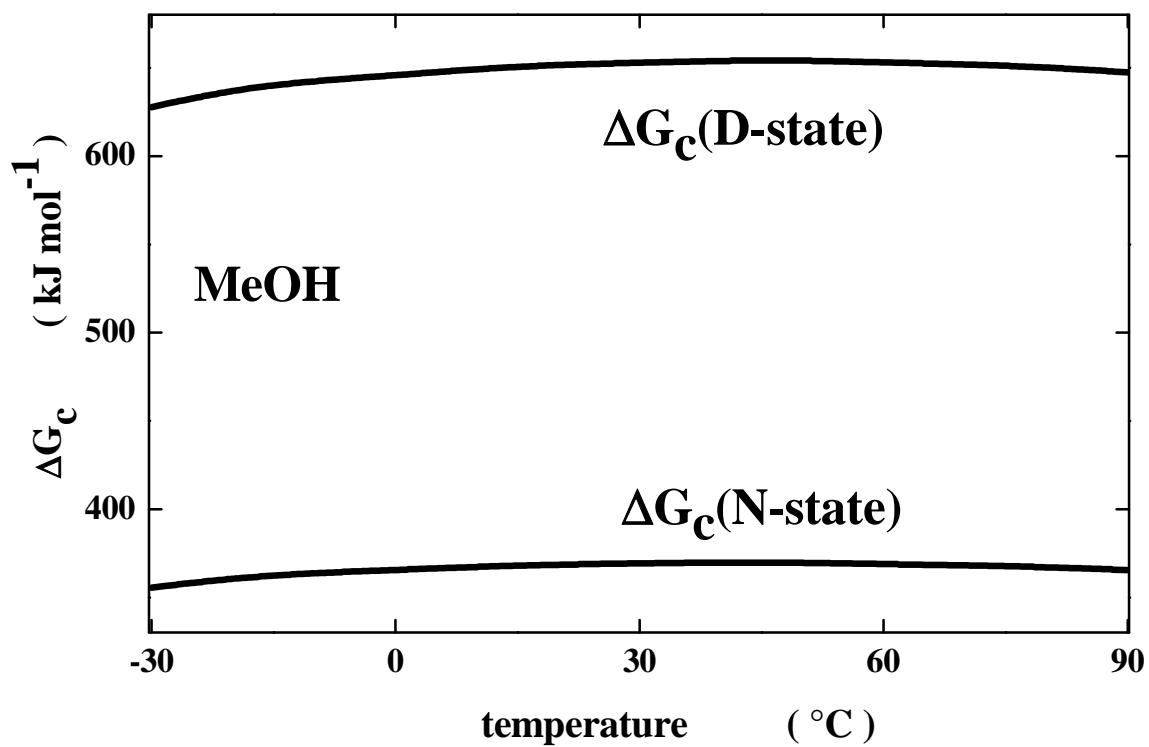
**Figure 4.** Temperature dependence of the  $\Delta G_c$  functions calculated in the aqueous 40% (by weight) MeOH solution for the spherical cavity corresponding to the N-state, and the spherocylindrical cavity corresponding to the D-state.

Figure 5.



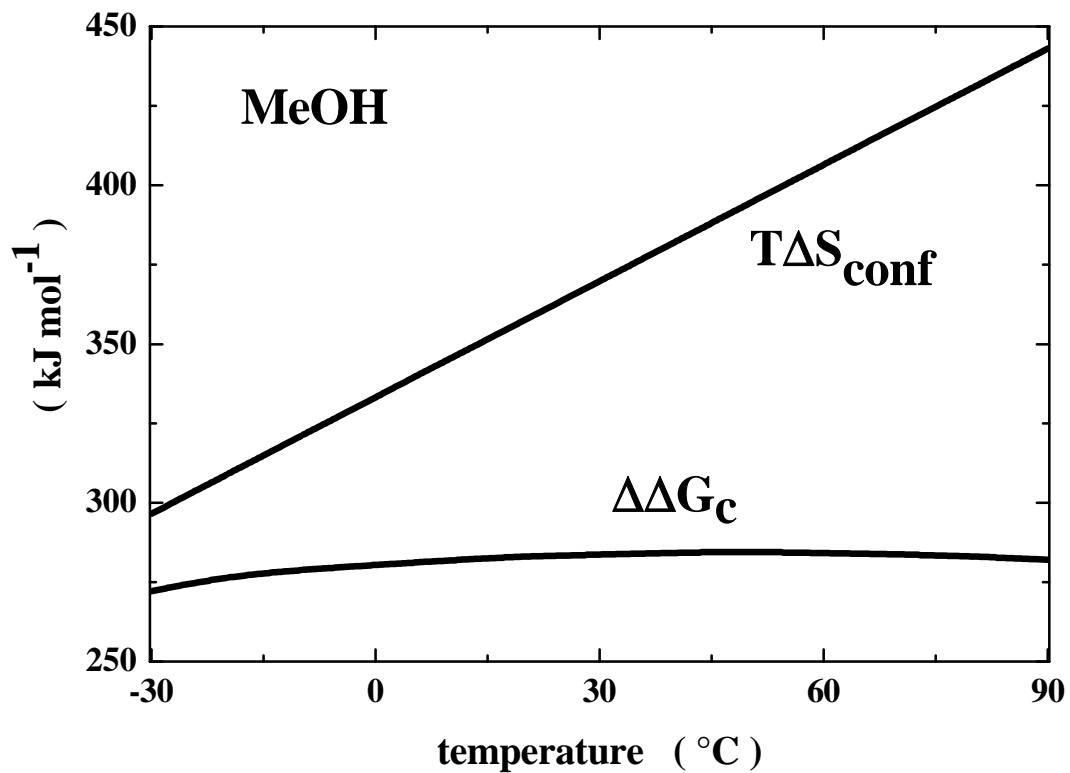
**Figure 5.** The curve  $\Delta\Delta G_c = \Delta G_c(\text{D-state}) - \Delta G_c(\text{N-state})$  of Figure 4 (40% MeOH in water) is shown together with the  $T\cdot\Delta S_{\text{conf}}$  straight line, calculated fixing  $N_{\text{res}} = 50$  and  $\Delta S_{\text{conf}}(\text{res}) = 24.4 \text{ J K}^{-1}\text{mol}\cdot\text{res}^{-1}$ .

Figure 6.



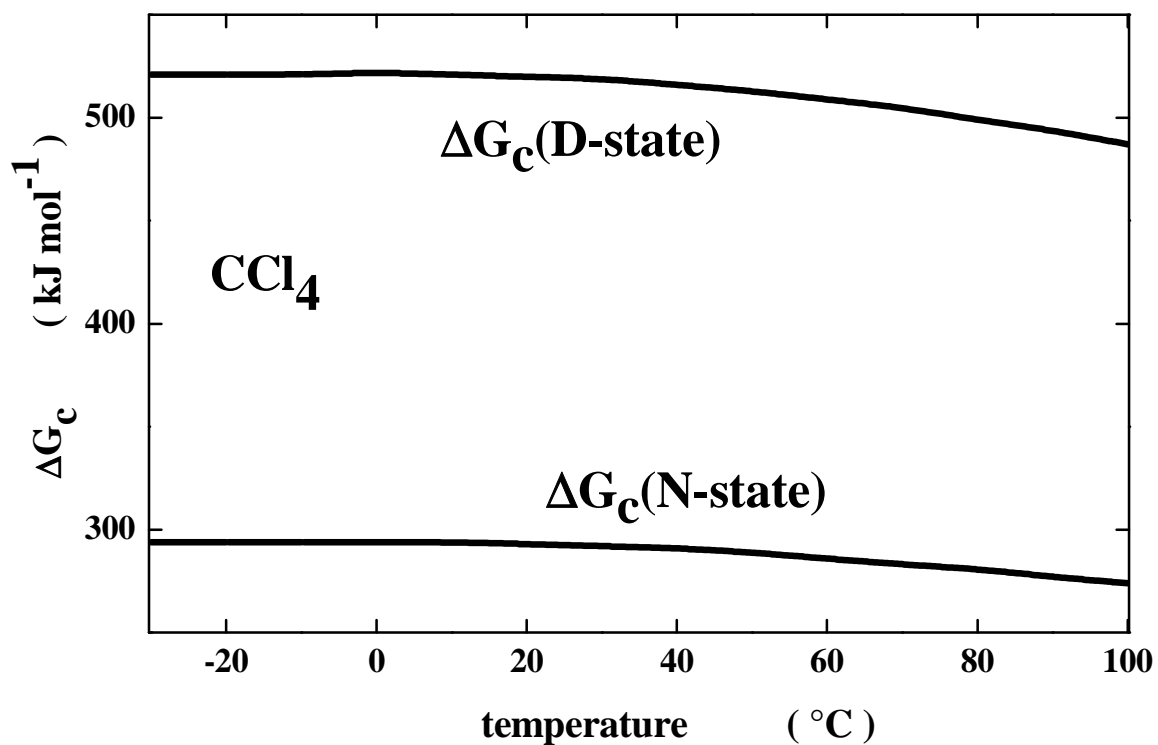
**Figure 6.** Temperature dependence of the  $\Delta G_c$  functions calculated in methanol for the spherical cavity corresponding to the N-state, and the spherocylindrical cavity corresponding to the D-state.

Figure 7.



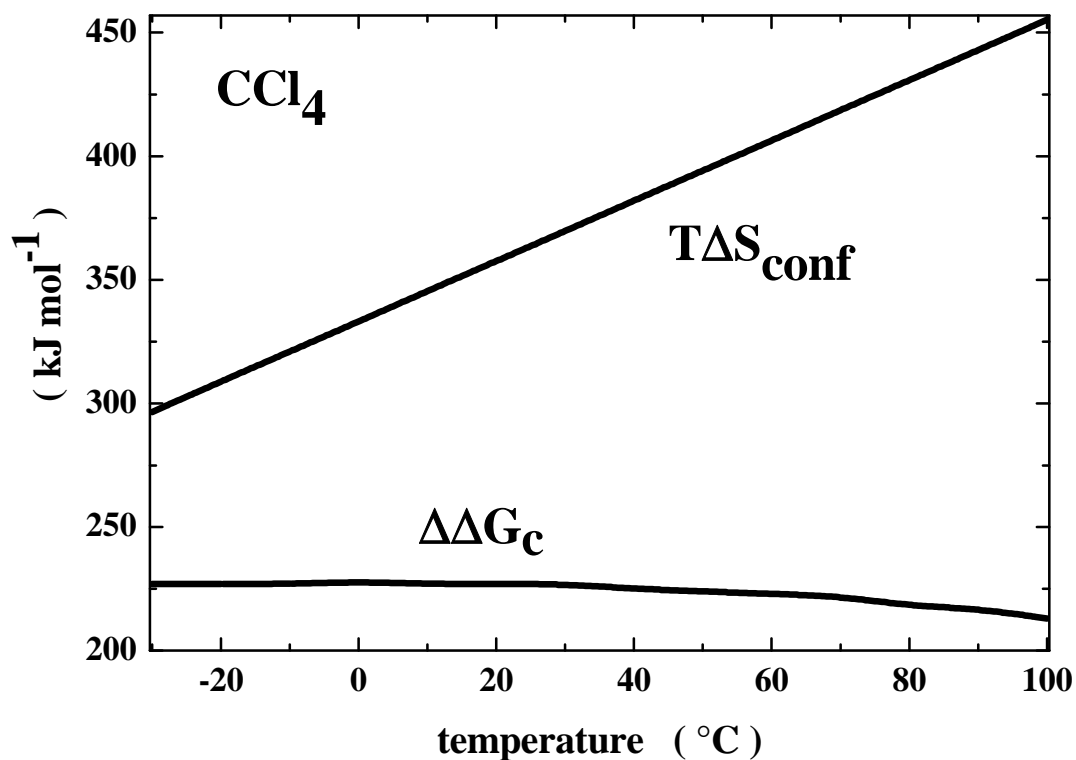
**Figure 7.** The curve  $\Delta\Delta G_c = \Delta G_c(\text{D-state}) - \Delta G_c(\text{N-state})$  of Figure 6 (methanol) is shown with the  $T\cdot\Delta S_{\text{conf}}$  line, calculated fixing  $N_{\text{res}} = 50$  and  $\Delta S_{\text{conf}}(\text{res}) = 24.4 \text{ J K}^{-1}\text{mol}\cdot\text{res}^{-1}$ .

Figure 8.



**Figure 8.** Temperature dependence of the  $\Delta G_c$  functions calculated in carbon tetrachloride for the spherical cavity corresponding to the N-state, and the spherocylindrical cavity corresponding to the D-state.

Figure 9.

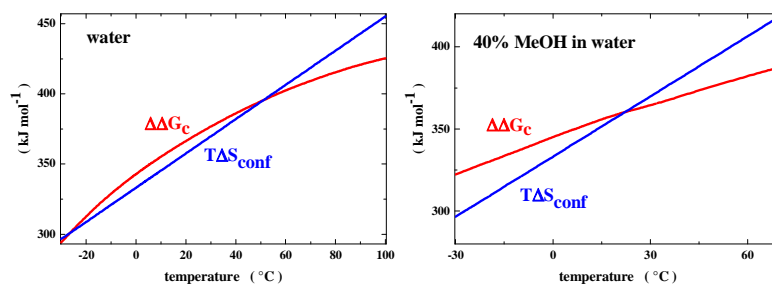


**Figure 9.** The curve  $\Delta\Delta G_c = \Delta G_c(\text{D-state}) - \Delta G_c(\text{N-state})$  of Figure 8 (carbon tetrachloride) is shown together with the  $T \cdot \Delta S_{\text{conf}}$  straight line, calculated fixing  $N_{\text{res}} = 50$  and  $\Delta S_{\text{conf}}(\text{res}) = 24.4 \text{ J K}^{-1} \text{ mol} \cdot \text{res}^{-1}$ .

## Table of Contents Entry

Manuscript title: On the mechanism of cold denaturation

Author: Giuseppe Graziano



The destabilizing contribution of chain conformational entropy intersects at two temperatures the stabilizing contribution of translational entropy of waters.